Review of Materials Research 1 (2025) 100009

Contents lists available at ScienceDirect

Review of Materials Research

journal homepage: www.sciencedirect.com/journal/review-of-materials-research

Multiscale characterization of three-dimensional printed silicone rubber: More insights from neutron scattering

Xiang Luo [a], Shengyi Zhong [b], Dong Liu [a,*]

[a] Key Laboratory of Neutron Physics and Institute of Nuclear Physics and Chemistry, China Academy of Engineering Physics, Mianyang, 621999, China
[b] School of Materials Science and Engineering, Shanghai Jiao Tong University, Shanghai, 200240, China

ARTICLE INFO

Keywords:
Three-dimensional printing
Silicon rubber
Microstructure
Material characterization
Neutron scattering

ABSTRACT

Three-dimensional printing technology provides substantial developmental advantages for silicone rubber, such as enhanced precision, the ability of fabricating intricate structures, and accelerated manufacturing processes. This review first offers an overview of 3D printing technology and its commonly used materials, with a particular emphasis on diverse materials introduced in recent years, especially those suitable for high-performance elastomers such as silicone rubber. It then comprehensively analyzes the characteristics, advantages, and challenges of 3D printed silicone rubber, including its processing adaptability and molding performance. A detailed discussion follows the characterization techniques, including mechanical testing, electron microscopy, thermal analysis, and scattering methods, which are used to evaluate the microstructure, mechanical properties, and thermal stability of the printed materials. Finally, the review explores the application of neutron scattering techniques in studying 3D printed silicone rubber, highlighting how these methods deepen the understanding of the material's microstructure, particularly in terms of polymer chain configuration and molecular dynamics. By integrating the latest advancements, this review aims to serve as a valuable reference for design, optimization, and industrial implementation of 3D printed silicone rubber.

1. Introduction

Three-dimensional printing, also known as additive manufacturing, is widely recognized as a transformative breakthrough in the manufacturing sector [1]. Initially developed in the late 1980s, it is a class of rapid manufacturing techniques that rely on computer-aided design (CAD) models to construct physical objects by sequentially depositing layers of materials such as powders, resins, or other bondable substances, as illustrated in Fig. 1. Compared to conventional manufacturing methods, 3D printing offers unparalleled design flexibility, allowing for the creation of complex geometries and fine feature dimensions without the need for molds or machining. This capability enables the production of highly precise and intricate structures, the simultaneous construction of multiple objects, and significant time and cost savings, thereby substantially improving production efficiency.

Currently, 3D printing technologies can be primarily classified into several major categories, including fused deposition modeling (FDM) [2], stereolithographic printing [3], selective laser sintering (SLS) [4], direct ink writing (DIW) [5], and so no. Each technique exhibits unique advantages and is tailored to specific applications. The choice of technology not only influences the geometric characteristics of the final product but also plays a pivotal role in shaping the material's microstructure.

Three-dimensional printing techniques are capable of fabricating a diverse array of materials, including metals [6,7], polymers [1,8,9], ceramics [10,11], and concrete [12,13]. Among them, silicone rubber stands out as a particularly promising material for both industrial and medical applications due to its outstanding flexibility, heat resistance, weatherability, and biocompatibility. As a result, it has garnered significant attention in the advancement of 3D printing technologies and holds considerable potential for future applications.

The core value of silicone rubber 3D printing technology lies in its ability to overcome the geometric constraints of traditional molding processes, enabling the integrated manufacturing of structure and function. Its applications can be categorized into three major domains: (1) Customized implants and biomimetic devices in the biomedical field. Such applications require materials with both high printing accuracy (micrometer feature size) and long-term internal stability, which makes it difficult for traditional silicone rubber to achieve complex internal cavity structures due to demoulding limitations. In 2020, Thomas et al.

* Corresponding author.
E-mail address: dongliu10@mail.ustc.edu.cn (D. Liu).

https://doi.org/10.1016/j.revmat.2025.100009
Received 21 March 2025; Received in revised form 3 April 2025; Accepted 4 April 2025
Available online 5 April 2025

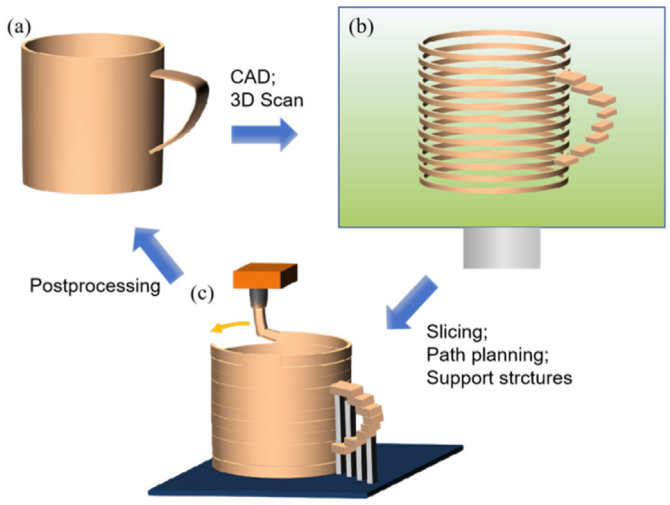

Fig. 1. Basic principles of additive manufacturing. (a) Development of product idea that is transformed into digital data by means of CAD, or analysis of geometric data by means of 3D scanning; (b) preprocessing of model data: slicing of virtual model into layered data, adjustment of support structures to stabilize craning structures, path planning, and successive transfer of layered data to 3D printer; (c) and additive manufacturing of model or product, for example, by melt extrusion, postprocessing to remove typical artifacts including support structures and surface roughness due to staircase effects [1]. Copyright 2017, Chemical Reviews.

developed compliant silicone scaffolds infused with cardiomyocytes (CMs), where a porous 3D-printed single-chain silicone scaffold exhibited a stiffness of 280 ± 40 kPa, closely matching that of human myocardium [14]. This material demonstrated promising potential as a functional myocardial patch for myocardial infarction treatment. In 2023, Duraivel et al. developed a support material formulated from a silicone oil emulsion, which exhibited negligible interfacial tension with photo-curable silicone-based inks. They successfully manufactured complex anatomical silicone rubber models, including brain vasculature, cerebral aneurysms, and aortic heart valves [15]. (2) Functional integrated device for flexible electronics and soft robots. These devices rely on 3D printing's micro-scale integration of heterogeneous material interfaces (silicone rubber-conductor), which cannot be achieved by traditional processes. In 2019, Yu et al. developed a polydimethylsiloxane (PDMS)-based photocuring elastomer with dynamic covalent cross-linking [16]. The elastomer is able to fully recover its original strength under mild conditions via disulfide exchange, and can be used to prepare self-repairing 3D soft actuators as well as self-repairing sensors with dielectric and conductive properties. Wang et al. proposed a printable diradical elastomer network based on a thiol−ene click chemical reaction as a material for wearable sensors. The material also has excellent flexibility (with an elongation of up to 1000 %), stability and weather resistance, and can work in harsh environments (−50 °C ~ 120 °C) [17]. Nevertheless, the viscoelasticity and specific curing requirements of silicone rubber present significant technical challenges for 3D printing. These characteristics also underscore the importance of structural characterization for gaining a comprehensive understanding of the quality and performance of printed products. This review will focus on the domain of 3D printed silicone rubber and introduce in detail the relationship between interlayer adhesion, internal stress, and microstructure of silicone rubber printing products and their macroscopic properties. Structural characterization techniques provide an important basis for optimizing process parameters and improving printing accuracy.

2. Three-dimensional printing materials

2.1. Oligomer and block polymer

The diversity of polymeric materials offers a broad selection for the fabrication of high-performance composites, while also serving as research and processing reference for the in-depth understanding of silicone rubber. Oligomer, as intermediate substances with molecular weights between monomers and high polymers, typically exhibit high processing fluidity, which enhances their performance in printing complex geometries. Additionally, the self-assembly behavior of block polymer can be leveraged to control structural phase separation in composite materials, facilitating the precise modulation of material properties.

In 2023, Catt et al. employed oligomers with three sequence-defined distinct sequence structures, namely alternating, triblock, and block structures, in 3D microprinting for the first time [18]. The differences in network topology resulting from the various sequence structures, as depicted in Fig. 2, subsequently influenced the mechanical and printing properties of the materials. The alternating arrangement of side chains forms a homogeneous network structure, which frequently leads to a higher elastic modulus for the printed microstructures. The dense arrangement of acrylate side chains may result in a high conversion rate of acrylate in local regions.

High molecular weight oligomers are often associated with high viscosity [19], which facilitates the formation of highly entangled polymer chains [20]. However, the traditional photocuring technique often requires the incorporation of reactive diluents when dealing with high-viscosity resins, which can lead to the degradation of material properties. Weng et al. developed a novel linear scan-based vat photopolymerization (LSVP) system that can effectively print ultra-high-viscosity ultraviolet (UV) curable resins with viscosities exceeding 600000 cps [21]. The LSVP system creates an isolated printing zone by using four rollers, allowing the resin to cure and separate simultaneously, thus overcoming the limitations of traditional UV curing techniques for high-viscosity resins. In 2024, Wei et al. developed a solvent-free photocurable resin that was made from a branched maleimide oligomer [22]. The structure of the resin allowed it to dissolve in photocurable monomers, resulting in a low-viscosity resin. The resin exhibited exceptional energy storage modulus, minimal shrinkage, and the ability to support heavy loads, and it enabled the printing of complex 3D structures with high resolution (50 μm).

In 2023, Goyal et al. successfully applied the DIW technique for the 3D printing of styrene-isoprene-styrene (SIS) copolymers. SIS, a thermoplastic elastomer (TPE), exhibits notable heat and weather resistance [23]. The SIS block copolymer printed via DIW demonstrated exceptional mechanical properties, including high tensile strength, elastic modulus, elongation at break, and toughness. In 2024, Kim et al. explored a novel 3D printed soft elastomer material based on physically cross-linked,

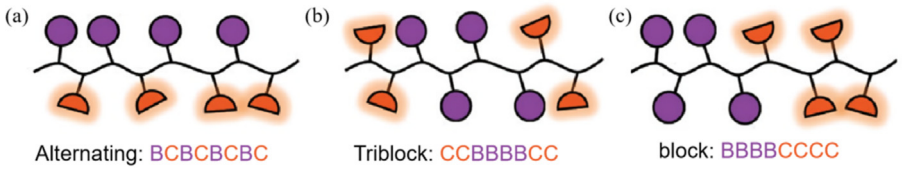

Fig. 2. The three target sequences: (a) alternating (BCBCBCBC), (b) triblock (CCBBBBCC), and (c) block (BBBBCCCC) to be used for printing [18]. Copyright © 2023, Small.

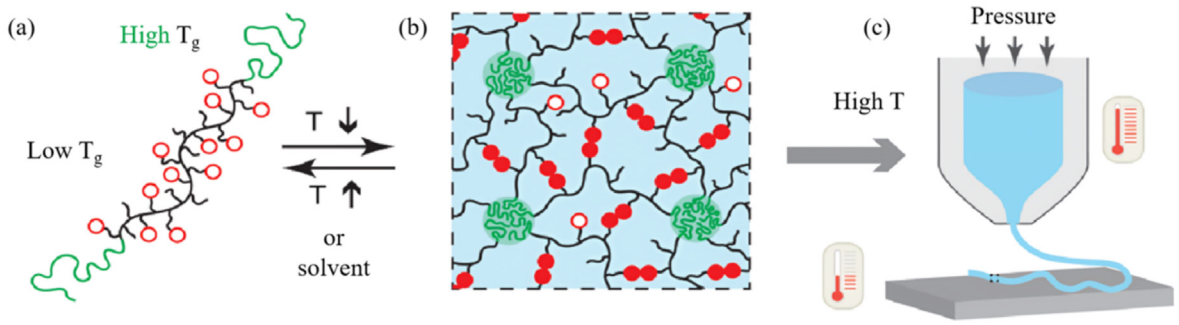

Fig. 3. DIW printable modular soft elastomer design concept. (a) Illustration of a linear-associative-linear (LAL) triblock copolymer. (b) At relatively low temperatures, the LAL triblock copolymer self-assembles into a microstructure. (c) In the network, the glassy domains effectively act as strong cross-links and maintain the material integrity upon deformation [24]. Copyright 2024, ACS Polymers Au.

homogeneously associated polymers [24]. This material consists of a linear-association-linear (LAL) triblock copolymer with tunable composition and proportions, wherein the midblock incorporates an associative polymer containing double hydrogen-bonded amide groups, and the terminal blocks form rigid, glassy domains that act as physical cross-links. The diagram and the printing process are shown in Fig. 3. The system allows for modular control over stiffness and toughness, offering precise regulation of energy dissipation.

2.2. Polymer complex

With the increasing complexity of application requirements, the performance of a single material often proves insufficient to meet diverse functional demands. Polymer complex, which involves the combination of different materials to improve mechanical strength, durability, and functionality, is the key direction of modern 3D printing technologies.

Three-dimensional printed polymer materials have made significant progress in recent years, especially in combining different polymers and functional materials, thereby imparting new properties and expanding the materials' potential applications. Wong et al. proposed a novel 3D printed hydrogel material composed of hydrophilic silicone resin, acrylamide (AA), and polyethylene glycol dimethacrylate (PEGDMA) [25]. This material exhibits superior mechanical properties and a high capacity for water absorption, closely mimicking the characteristics of human cartilage while maintaining biocompatibility with human tissues. It overcomes the limitations of traditional silicone resin materials, such as high viscosity and strong hydrophobicity, enabling the fabrication of bioinspired structures with enhanced mechanical performance and biocompatibility. In 2024, Xu et al. presented an innovative approach for 3D printed high-strength silicone-based polyurethane-polyurea (PSURA). They printed the acrylate-terminated polysiloxane-based polyurethane (PSUA) prepolymer with favorable fluidity into the requisite 3D structure and cured it via ultraviolet irradiation [26]. Following the curing process, the printed structure was immersed in a chain extender solution, facilitating the reaction of residual isocyanate groups with the chain extender, ultimately forming a cross-linked polymer network. The tensile strength and elongation at break of the material have been enhanced by 330 % and 60 %, respectively, demonstrating outstanding energy dissipation capacity.

3. Three-dimensional printed silicone rubber materials

As 3D printing technology expands into biomedical and flexible electronics applications, traditional polymers increasingly show limitations such as narrow mechanical properties and insufficient biocompatibility. Due to the high viscoelasticity of silicone rubber at room temperature, mainly adopts DIW technology based on shear thinning effect, which requires precise control of the interaction between rheological modifiers (such as fumed silicon dioxide) and the matrix in the material formulation. Compared to laser melting for metals or melt extrusion for thermoplastics, the additive manufacturing of silicone rubber places greater emphasis on the control of viscoelasticity and post-curing process optimization. While silicone rubber offers superior structural performance and cross-disciplinary application potential, it also presents challenges in the standardization of processing techniques and material formulations, necessitating further advancements in both technical protocols and regulatory frameworks.

3.1. Silicone rubber raw materials

3.1.1. Raw rubber

Un-vulcanized raw silicone rubber, primarily composed of Si-O-Si bonds and side-chains organic groups, is soft and viscous, which limits its mechanical properties, including elasticity, heat resistance, and aging stability, as compared to fully vulcanized silicone rubber. Upon vulcanization, this material becomes suitable to produce a wide array of silicone rubber products, such as sealing rings, catheters, sealing materials for medical and electronic devices, and automotive seals. In the context of 3D printing, unvulcanized silicone rubber can also be processed through specialized extrusion or melt deposition techniques to fabricate high-precision silicone rubber components. In 2023, Garcia et al. examined the feasibility of DIW using styrene-butadiene rubber (SBR)-based sealants as raw materials [27]. The study revealed that, in comparison to traditional SBR materials, 3D printed SBR does not necessitate vulcanization, offers reduced production costs, and demonstrates favorable mechanical and rheological properties.

3.1.2. Fillers

Silicone rubber without filler reinforcement typically exhibits subpar mechanical properties, necessitating the incorporation of reinforcing fillers to enhance its performance for a wide range of applications. Commonly used reinforcing fillers include titanium dioxide, silica (white carbon black), graphene, carbon black, and calcium carbonate, among others. [28–30]. Furthermore, certain functional fillers can impart specific physical or chemical properties to silicone rubber, such as enhanced compressibility, durability, and hydrophobicity [31], broadening its applicability across a diverse range of scenarios. In 2018, Porter et al. found that the addition of carbon black can effectively solve the problems of sagging, nozzle blockage, and electrostatic repulsion of silicone during the additive manufacturing printing process of UV-cured silicone [32]. Their findings identified an optimal CB loading of 0.15 wt%, which effectively reduces the repulsive effect while maintaining hardness and modulus properties close to those of bulk materials. Wang et al. combined polydimethylsiloxane (PDMS) composite materials with carbon nanotubes (CNTs), to fabricate three-dimensional composite materials and successfully constructed a conductive CNTs network to manufacture conductive flexible materials with self-healing function [33]. The material demonstrated the ability to self-repair cracks under electrothermal or photothermal stimulation.

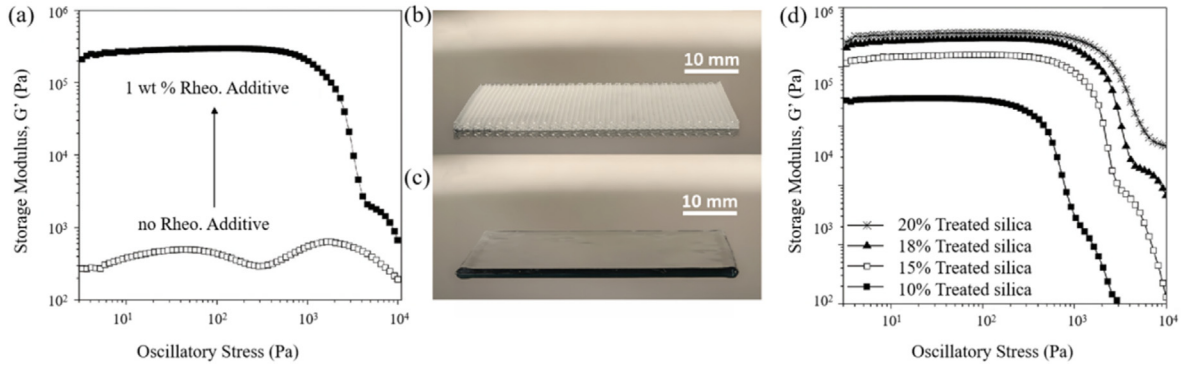

Fig. 4. The effect of rheological modification additives on 3D printing after adding them to the filled silica gel dispersion. (a) The storage (G') modulus of silicone inks without or containing 1 wt% rheological additives. (b) Three-dimensional printed lattices (8-layer FCT structure) containing 1 wt% rheological additives. (c) The same crystal lattice as in (b), printed with silicone inks without rheological additives ($G'' > G'$). (d) Effect of treated reinforced silicon filler [34]. Copyright 2018, Macromolecular Rapid Communications.

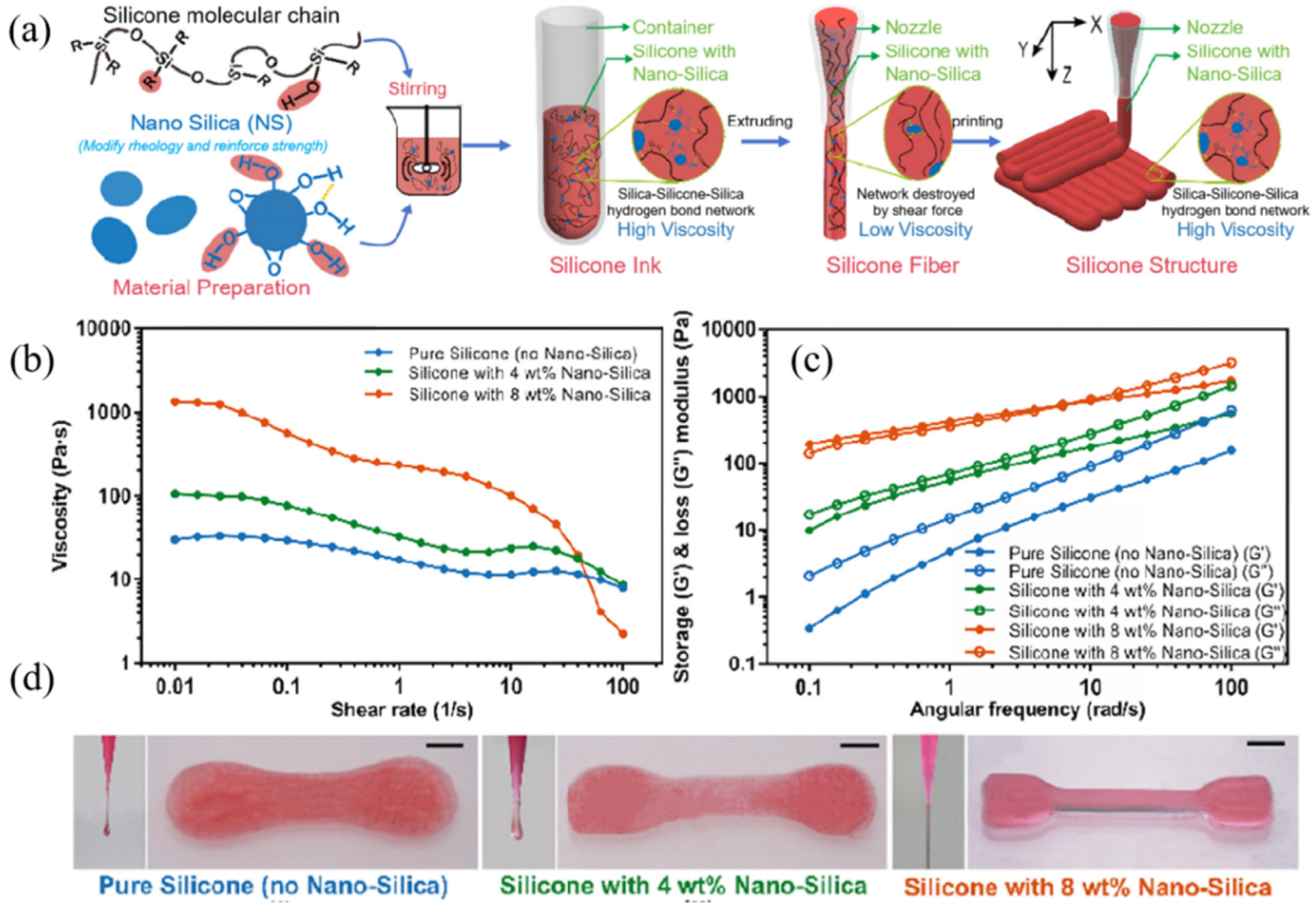

Fig. 5. Principle and implementation of 3D printing of silicones. (a) Rheological modification mechanism of silicone rubber; (b) steady-shear and (c) oscillatory conditions for inks withincreasing concentration of 0, 4, and 8 wt % NS. (d) Optical photograph of the extruded fiber and printed structure using silicone inks with different components. (Scale bar, 5 mm). [37]. Copyright 2019, ACS Appl. Mater. Interfaces.

Additionally, modified fillers also play an important role in improving the mechanical properties, processing adaptability, and functionality of silicone rubber in the 3D printing process. In 2017, Durban et al. adjusted the rheological properties and stability of the ink by adding hexamethyldisilazane-treated (HMDZ) silica to vinyl terminated poly(-dimethylsiloxane)-*co*-(diphenylsiloxane) (PDMS-*co*-PDPS) and rheology modifying additives [34]. Rheological analysis revealed that the inclusion of rheology-modifying additives at varying concentrations notably improved the pseudoplastic behavior of the ink, facilitating the development of an elastomer with tunable hardness. As illustrated in Fig. 4, the addition of rheology modifying additives in the presence of silica filler results in a highly pseudoplastic material characterized by a significant yield stress, attributed to the formation of a stable three-dimensional network between the filler and the additive.

The type and concentration of fillers can adjust the viscosity and rheological properties of the ink, thereby improving both the precision and stability of the printing process, while preventing issues such as collapse or uneven flow. However, the incorporation of fillers typically results in an increase in viscosity, making it essential to carefully balance the trade-off between reinforcement and viscosification.

3.2. Three-dimensional printed silicone rubber design performance

3.2.1. Rheology-based ink design and properties

Rheology-based ink formulation and characterization primarily focus on the flow behavior, viscosity, shear stress, and shear rate of the ink during the printing process [34–36]. The rheological properties of ink are largely influenced by its microstructure, which is intricately linked to various structural factors, including particle morphology, particle size distribution, the extent of polymer chain cross-linking, as well as the type and distribution of fillers. These structural attributes substantially impact the viscosity, elastic modulus, and flow behavior of the ink. Collectively, they govern the fluidity and stability of the ink throughout the printing process and, in turn, influence the mechanical properties of the final printed product.

Silicone exhibits inherently favorable adjustable viscosity and rheological properties, making it well-suited for the DIW technique. To overcome the challenges associated with low viscosity and extended curing times in silicone, Zhou et al., introduced nano-silica (NS) as a rheological modifier [37]. Incorporation of NS significantly altered the rheological behavior of silicone, transitioning it from a purely Newtonian fluid to a viscoelastic material, exhibiting a distinct shear-thinning effect [38]. The modification resulted in a significant increase in low-shear viscosity, improving the controllability of the printing process. The mechanism of rheological modification of silicone rubbers is shown in Fig. 5a. Upon the addition of NS, the rheological behavior of the fluid transitions from that of a purely Newtonian fluid to one exhibiting a pronounced shear-thinning effect, as illustrated in Fig. 5b. Increasing the NS concentration from 0 to 8 wt% leads to a two-order-of-magnitude increase in low-shear viscosity, progressively shifting the system from a sol state to a gel state, as depicted in Fig. 5c. Inks with different NS concentrations are extruded to form fibers and print structures. The results show that the viscoelastic properties of high NS concentration inks are key to preventing deformation of printed objects (Fig. 5d). The increase in viscosity is primarily attributed to the formation of a three-dimensional network, facilitated by the "bridging" interactions between silica and silicone. Under shear stress, these network connections are disrupted, causing a reduction in viscosity. Conversely, the reformation of these bonds upon the cessation of shear stress contributes to viscosity recovery. This alteration in the material's microstructure significantly impacts its macroscopic rheological behavior.

In certain applications, such as the printing of long-span structures, the material may still collapse under the influence of gravity or compression forces. To address the limitations of traditional silicone inks, which fail to maintain structural integrity during printing, Geng et al. introduced a UV-curable rheological modifier into the ink, effectively mitigating this issue [39]. The effects of silica and AS on the rheological and mechanical properties of silicone are illustrated in Fig. 6a–c. The incorporation of silica leads to an increase in viscosity and induces shear-thinning behavior, which is beneficial for DIW printing. As the silica concentration increases, the material transitions from a liquid-like state (where $G' < G''$), at 7 wt% silica) to a solid-like state (where $G' > G''$), at 14 wt% silica) under low oscillatory stress, facilitating better print fidelity. In addition, a small amount of AS forms a cross-linked network before UV irradiation, leading to an increase in viscosity and yield stress of the silica ink, and is solidified by UV light to avoid the collapse of the printed structure further, as shown in Fig. 6d–f.

In 2018, Zheng et al. reported a new method for 3D printing using a

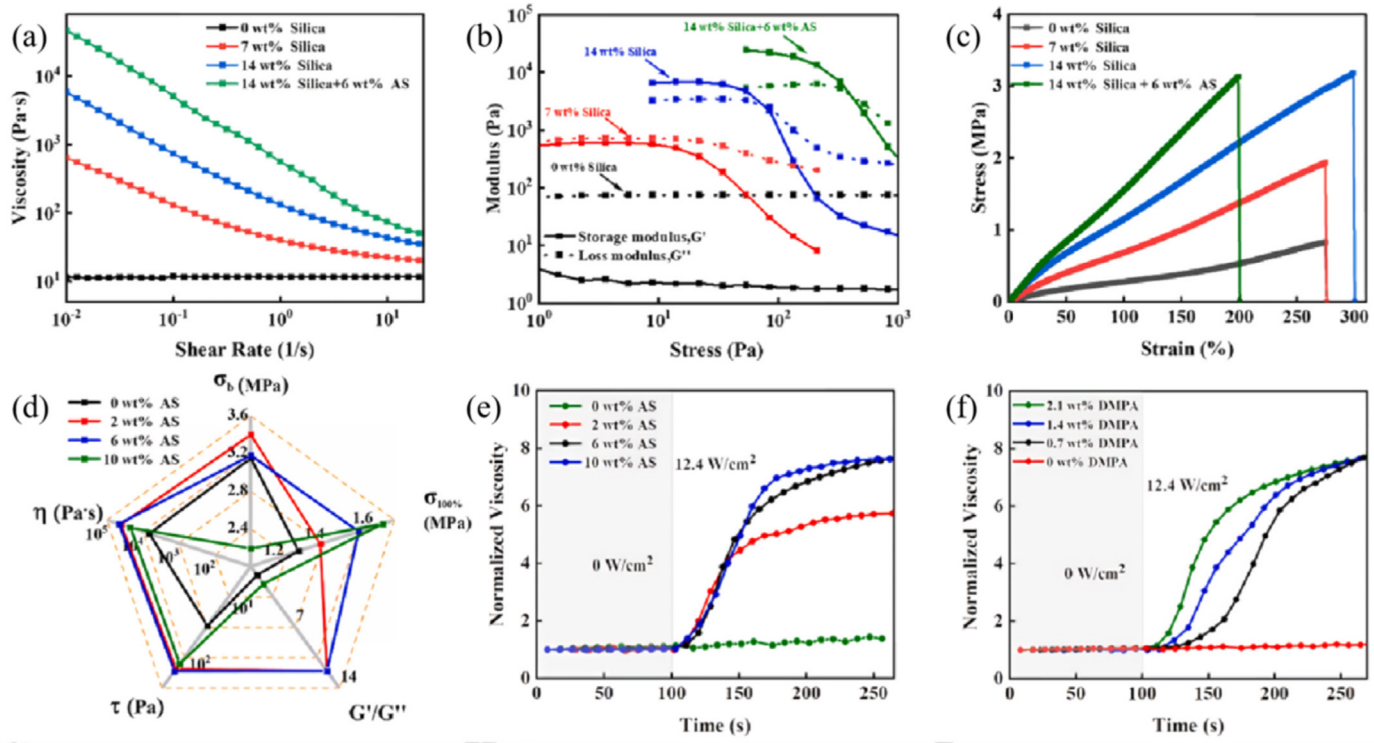

Fig. 6. Rheology and printability of the inks with different silica and AS contents. (a) Viscosity as a function of shear rate; (b) storage (G′) and loss modulus (G″) as a function of oscillatory stress; (c) Tenile stress-train curves for the cured elastomers; (d) Viscosity at the shear rate of 0.01/s, yield stress (τ), G′/G″ at the oscillatory stress of 1 Pa, stress at 100 % strain ($\sigma_{100\ \%}$) and break strength (σ_b) for the formulations with 14 wt% silica and different AS contents; (e) UV assisted viscosity change for the inks with 14 wt% silica and different AS contents; (f) UV assisted viscosity change for the inks with different DMPA solution (UV initiator) contents [39]. Copyright 2024, Composites Part B.

low-viscosity silicone ink (viscosity <2000 cSt) which employs thiol-ene "click" chemistry for the rapid fabrication of multi-material structures [40]. During the curing process, the addition of chain extender makes the ink form high molecular weight polymers, which subsequently form a cross-linked network. This network not only enhances the mechanical strength of the material but also increases its elasticity.

Moreover, certain models provide valuable insight into the rheological behavior of inks [41,42]. In 2021, Shao et al. applied the Finite Extensible Nonlinear Elastic-Peterlin (FENE-P) model to describe the viscoelastic behavior of dilute solutions [43]. By accounting for the elasticity of polymer chains and their interactions in solution, this model effectively simulates the flow and recovery characteristics of the ink under shear or tensile stresses. Their fitting results indicated that the expansion rate of nano-silica-reinforced silicone rubber ink is directly proportional to the relaxation time of the ink. This correlation is attributed to the inclusion of nano-silica which enhances the ink's elasticity, promoting greater expansion during the extrusion process when the relaxation time is longer.

To fully understand the macroscopic performance of materials, it is essential to investigate their underlying rheological properties. By examining how materials behave under various flow and deformation conditions, valuable insights can be gained regarding their performance characteristics. The realization not only aids in optimizing material formulation but also enhances our ability to predict how materials will respond in practical applications. However, within the community, rheological studies often emphasize the rheological phenomena themselves, with limited focus on the associated structural information. Many studies are predominantly concerned with ontological relationships, model fitting, and qualitative analysis, while the connection between rheological behaviors and microstructure remains insufficiently explored.

3.2.2. *Post processing and properties*

As a type of silicone material, 3D printed silicone rubber usually requires further curing either during or after the printing process. In the course of curing, the molecular chains of silicone rubber undergo cross-linking, transforming the material into a solid form with enhanced elasticity and durability. Common curing methods include thermal curing [44], UV/laser curing [45], among others. In 2024, Ding et al. achieved UV-induced curing in the material extrusion printing process of platinum-catalyzed hydrosilylation silicone composites [46]. This approach significantly improved the shape retention of the material, ultimately enhancing its mechanical properties. The tensile properties of the printed Pt-catalyzed silicone composite fibers, cured by different methods, are shown in Fig. 7. Compared to thermal curing, UV-curing resulted in smaller pores, leading to improved isotropy in the material's mechanical properties. This method effectively resolves the trade-off between high yield stress and ink extrusion in the printing process, showing potential for developing high-performance 3D printed silicone. In 2021, Woo et al. demonstrated that the mechanical properties of porous PDMS are precisely tailored by adjusting structural parameters such as print shape and filling density [47]. The PDMS ink used in their study contained dibutyl phthalate (DBP), and porosity was achieved by removing DBP from the cured matrix. In comparison to non-porous PDMS, the resulting porous PDMS exhibited customizable two-dimensional or three-dimensional architectures, along with enhanced toughness, stiffness, strength, and ductility.

During the molding and processing of 3D printed silicone rubber, microstructural evolution often occurs, prompting further research into the relationship between the microstructure of materials and their macroscopic properties. The controllability and enhanced mechanical properties of porous PDMS offer new opportunities for the design of complex flexible devices. However, structural characterization

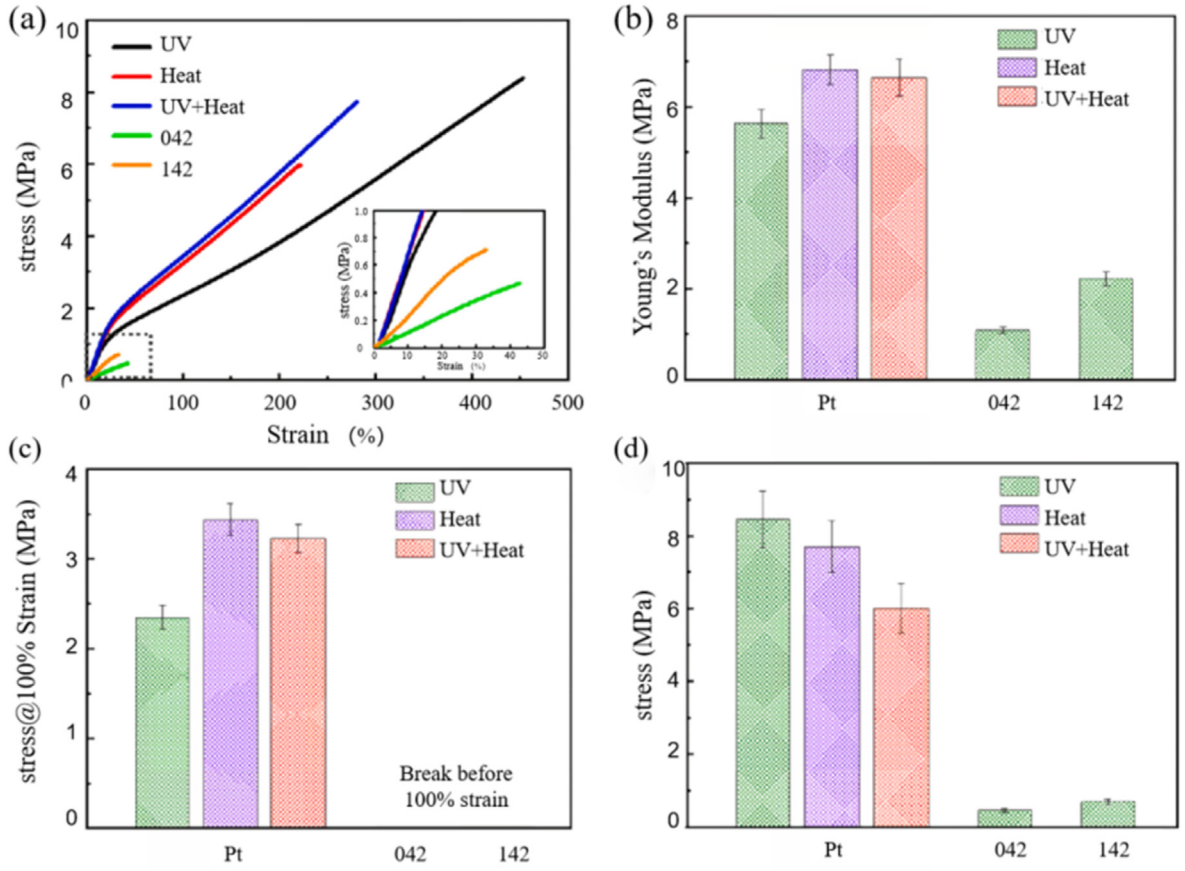

Fig. 7. Tensile properties of the printed Pt-catalyzed silicone composite fibers cured by different methods, and the control samples (042 and 142) cured by UV induced thiol-ene click reactions. (a) Typical tensile stress-strain curves; (b) Young's modulus ($n = 5$); (c) stress at 100 % strain ($n = 5$); (d) tensile strength ($n = 5$). The inset in (a) is an enlarged figure of the dashed area in the low strain range below 50 % [46]. Copyright 2024, Additive Manufacturing.

techniques are crucial for achieving high-precision fabrication and enabling the customized manufacturing of these materials.

4. Characterization methods for 3D printed silicone rubber materials

Various microscopic, spectroscopic, scattering, and mechanical testing techniques have been employed to investigate the structure, dynamics, mechanical properties, printing accuracy, and formation mechanisms of 3D printed silicone rubber. The selection of specific characterization methods depends on the requirements of the study, including factors such as the geometry of the printed model, the desired resolution, dynamic stress-strain behavior, and the specific physico-chemical and material properties of interest. At present, one of the key challenges in the development of silicone rubber nanocomposites remains the relationship between micro- and mesoscopic multi-scale structure and macroscopic properties of formulated materials under service conditions. The reinforcing fillers introduces a complex multi-component, multi-level system, primarily consisting of a filler network, a bonding network, and a polymer matrix network, each of which influences the material's final properties. This section provides an overview of several common characterization techniques used to examine the microstructural dynamics and mechanical properties of 3D printed silicone rubber. These techniques enable researchers to gain a comprehensive understanding of the material's properties, ensuring its reliability and long-term performance across diverse application scenarios.

4.1. Mechanics testing

Mechanical testing serves as a pivotal approach for assessing the static

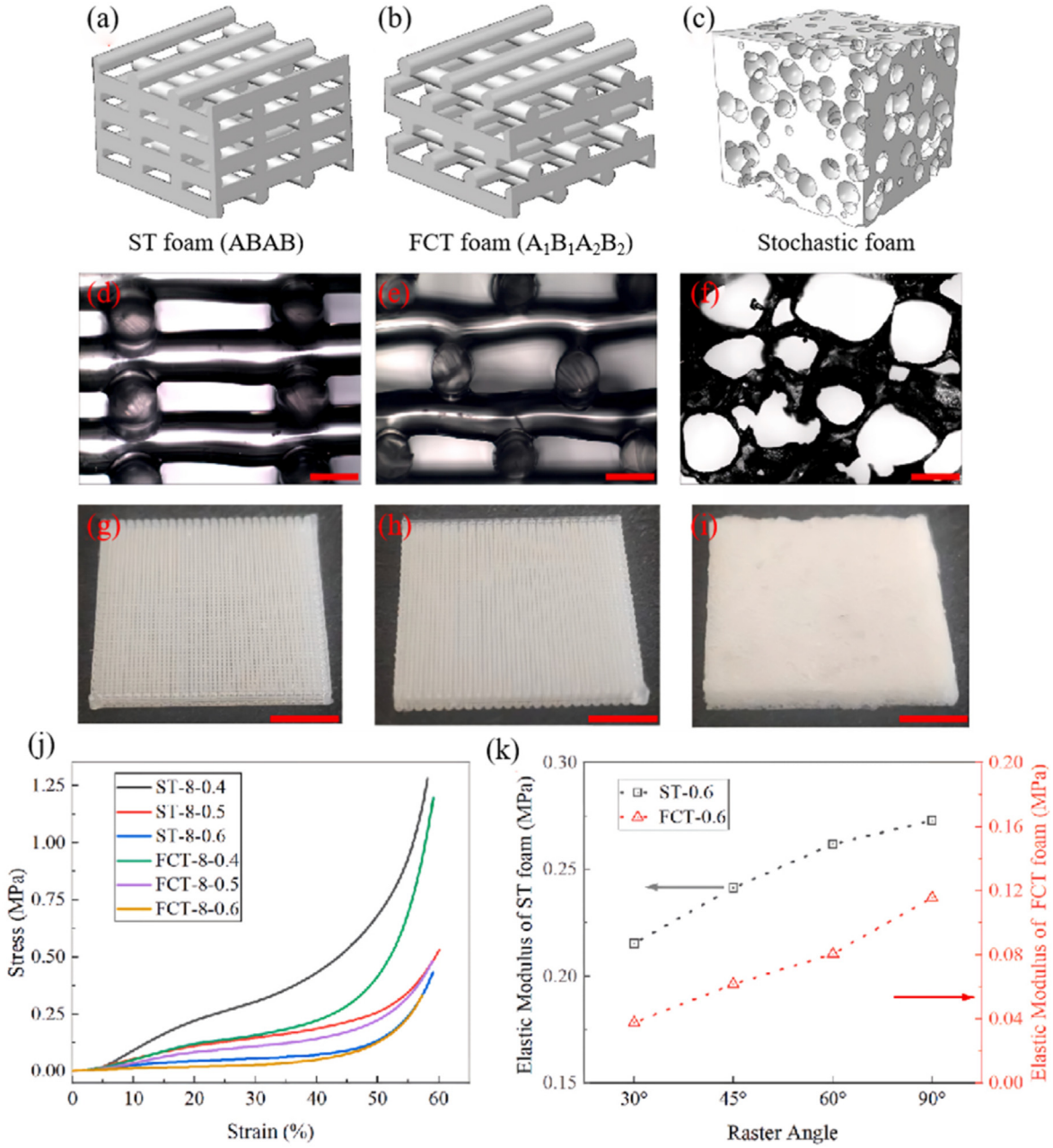

Fig. 8. Three types of silicone rubber foams with a density of 0.32 g/cm3 (a–c) Schematic diagrams, (d–f) cross-sectional optical micrographs, and (g–i) photographs of 3D printed foams with ST and FCT structures and traditional stochastic foam (the scale bars are 200 μm in d-f and 5 mm in h-j). (j) Compressive stress–strain curves of with ST and FCT foams; (k) effect of Raster Angle on elastic modulus of with ST and FCT foams [51]. Copyright 2023, Composites Communications.

mechanical properties of 3D printed silicone rubber materials. Mechanical tests include tensile, compression, shear, and other forms that provide key mechanical parameters such as elastic modulus, yield strength, and fracture strength. These parameters are crucial for understanding the rigidity, toughness and load-bearing capacity of materials in practical applications. Previous studies have shown that the mechanical properties of silicone rubber are affected by a variety of factors, including structure, cross-linking density, the introduction of fillers and external environmental conditions [14,48,49]. In 2014, Duoss et al. reported that "simple cubic" (SC)-like structure and "face-centered tetragonal" (FCT) configuration exhibit different load-responsive and direction-dependent behaviors, and that their mechanical properties are controlled by an orderly array of submillimeter pillars [50]. In 2023, Zhu et al. conducted a pioneering study on the stress relaxation behavior of 3D printed silicone rubber foams with varying topologies under uniaxial compression [51]. Using a universal testing machine (CTM4304S, MTS Corp., China), they evaluated polydimethylsiloxane (PDMS) foams with two distinct structural configurations: simple tetragonal (ST) and FCT structures, as shown in Fig. 8a and b. The stress relaxation characteristics were assessed by monitoring the temporal evolution of compressive stress and calculating both the compressive stress relaxation rate $\Phi(t)$ and the load retention rate $R(t)$. FCT foam exhibits a more uniform stress distribution and bending deformation during compression, while ST foam undergoes uniaxial buckling, leading to localized stress concentrations.

Recent years have witnessed significant advancements in printable polymer composites, with mechanical testing emerging as a powerful tool to facilitate their research and development [52–54]. In 2018, Huang et al. demonstrated a 3D printing method for fabricating conductive silicon rubbers (CSRs) that exhibited enhanced tensile strength, greater elongation at break, and increased Young's modulus when stretched along the orientation direction [55]. They successfully developed sandwich-type strain sensors based on the electrical response of CSRs subjected to varying mechanical loads.

Different from traditional mechanical testing methods, dynamic mechanical analysis (DMA) enables the assessment of the viscoelastic properties of materials by measuring their response under dynamic loading conditions. This technique allows for the evaluation of critical parameters such as the storage modulus, loss modulus, and loss factor [56], and is frequently used to determine the glass transition temperature of silicone rubber [48,57,58]. However, while experimental approaches provide valuable insights into the material's mechanical behavior, they are typically constrained by a single loading condition and test configuration, which limits their ability to capture the full complexity of material behavior under diverse operating conditions. In contrast, finite element analysis (FEA) offers a powerful complement to traditional experimental methods by enabling the numerical simulation and prediction of material responses across a wide range of loading scenarios. This approach is particularly beneficial when studying materials like silicone rubber, which exhibit highly nonlinear behavior and large deformations. FEA facilitates a more accurate representation of stress-strain distributions and relaxation phenomena, thereby enhancing the understanding of material performance under various conditions [51,59,60].

4.2. *Real space observation (electron microscopy)*

Optical microscopy provides a straightforward means for macroscopic observation of the structural features of 3D printed silicone rubber, including parameters such as line diameters, cross-sectional areas, layer stacking patterns, interlayer adhesion, and the presence of localized defects. Electron microscopy is often used to analyze the microstructure and form quality of silicone rubber. As shown in Fig. 9, Huang et al. observed silica tightly bound to rubber through TEM and AFM in the study of the mechanism of filler-rubber interaction [61]. High-resolution imaging techniques enabled the researchers to discern the fine structural

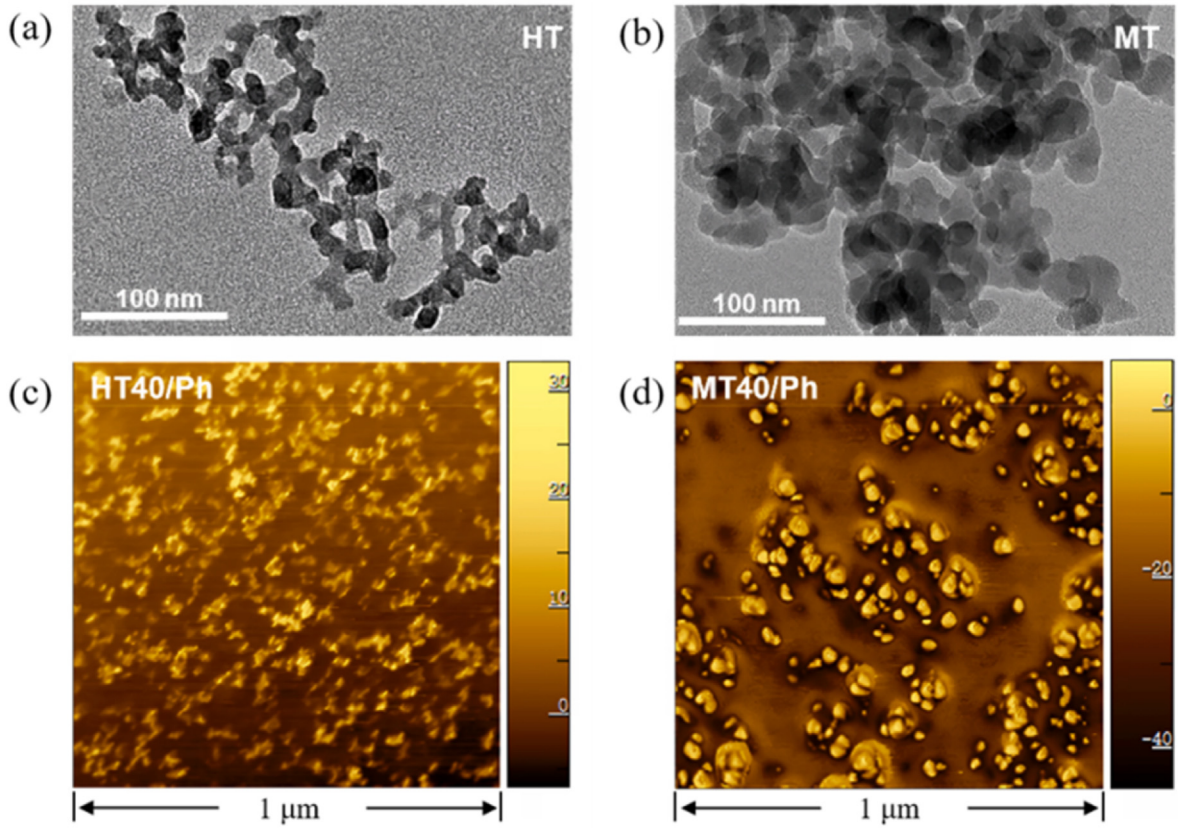

Fig. 9. TEM images of (a) HT fumed silica and (b) MT precipitated silica. AFM phase images of (c) PDMMPS filled with 40 phr HT precipitated silica (HT40/Ph) and (d) PDMMPS filled with 40 phr HT precipitated silica (MT40/Ph) [64]. Copyright 2023, Composites Science and Technology.

characteristics of silicone rubber, such as the polymer chain arrangement, filler distribution, and defect types. Furthermore, electron microscopy images serve as a valuable tool for uncovering the interactions and interfacial characteristics within 3D printed silicone rubber [62].

4.3. Spectral and thermal analysis

Spectral and thermal analysis represent effective approaches for assessing the chemical composition and thermal characteristics of 3D printed silicone rubber [17,63,64]. Techniques such as Fourier transform infrared (FTIR) spectroscopy and Raman spectroscopy provide insights into the molecular structure of materials, enabling the identification of chemical compositions and the elucidation of reaction mechanisms. Concurrently, thermogravimetric analysis (TGA) and differential scanning calorimetry (DSC) are utilized to investigate the thermal stability and phase transition characteristics of silicone rubber. In 2021, Foerster used FTIR-ATR spectroscopy to examine molecular structural changes induced by state transitions before and after curing, confirming the occurrence of crosslinking reactions. Additionally, DSC was used to study the curing behavior and glass transition in UV-cured silicon-based materials, which exhibit tunable mechanical properties by varying the proportion of polymerizable reagents [65]. Their findings indicated that variations in crosslinking density within the cured material led to alterations in the mechanical properties of the components. In a separate study, Walker et al. focused on enhancing the reliability of 3D printed silicone components by analyzing the interfacial bond strength during the DIW process [66]. Through DSC and peel tests on silicone formulations, they quantified the relationship between curing kinetics and bond strength, as shown in Fig. 10. Their research emphasizes the critical role of interfacial bonding in determining the structural integrity and tensile strength of soft, elastic silicone components, with relevance to applications such as soft robotics, where tensile forces are a key consideration.

These methods primarily focus on chemical composition and macroscopic thermal properties of materials, but they offer limited capability for directly observing the distribution, orientation, and interfacial interactions of fillers within the matrix. Consequently, these

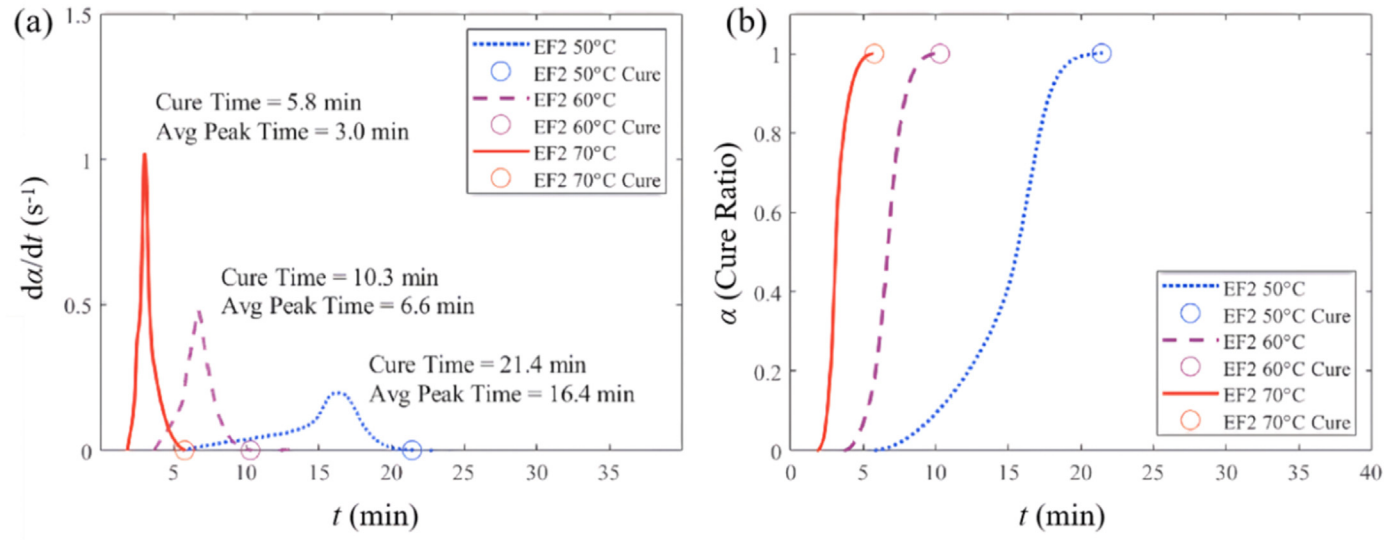

Fig. 10. Curing kinetics results measured by isothermal DSC testing. (a) Averaged isothermal scans of Ecoflex (EF) with cure time (noted on the graph with circles) and peak cure rate time. (b) Cure percent of EF vs. time, cure time noted on the graph with circles [66]. Copyright 2021, Additive Manufacturing.

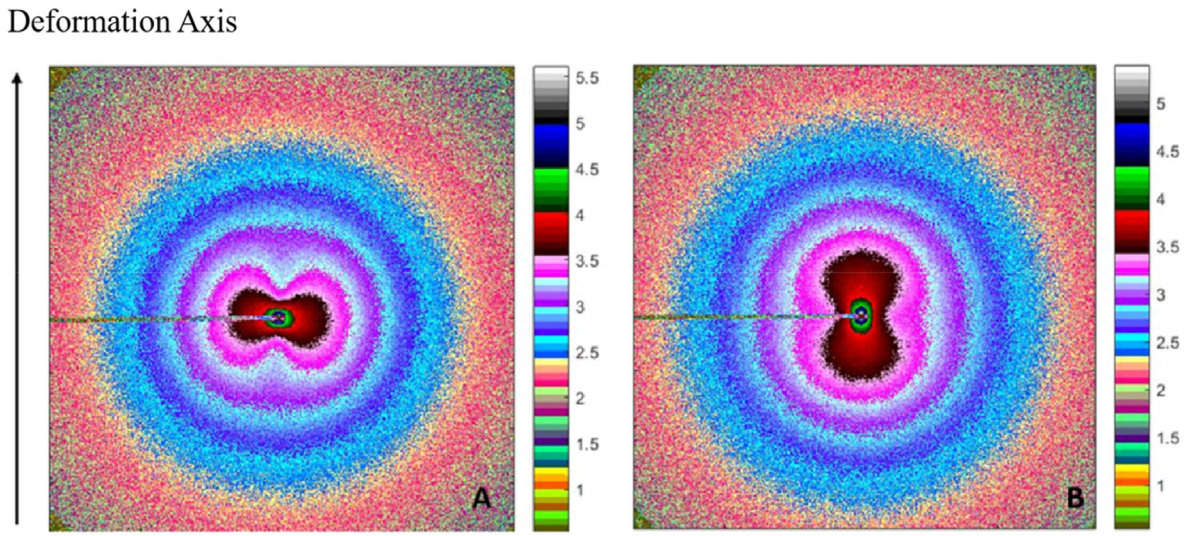

Fig. 11. Selected 2D initial raw scattering patterns for SSBR-90 phr Zeosil 1165 MP SiO_2. (A) (left) and (B) (right) represent two different positions of the same sample in the q-range ~2×10^{-4} to 0.01 $Å^{-1}$. The chosen color map was optimized to stress the changes to the butterfly shape and does not reflect a suggested oscillatory pattern [72]. Copyright 2019, Macromolecules.

techniques are not ideal for analyzing the formation process of layered structures or the evolution mechanisms of nanoscale filler networks. In this regard, scattering techniques such as X-ray scattering and light scattering serve as valuable complements, providing deeper insights into the microstructural characteristics of silicone rubber systems.

4.4. Dynamic light scattering and X-ray scattering

Scattering techniques are pivotal in the structural characterization of 3D printed silicone rubber, particularly dynamic light scattering (DLS) and small angle X-ray scattering (SAXS). DLS is commonly employed to study nanoparticles or colloidal systems in solutions making them suitable for examining particle size, distribution, and dispersion within filled silicone rubber [67,68]. SAXS, on the other hand, provides valuable information about the microstructure of the material, including nanoscale morphology, particle size, and shape [69].

In 2019, Shmueli et al. applied *in situ* wide-angle X-ray scattering (WAXS) to investigate extrusion-based 3D printing processes for various materials [70]. Their findings highlighted the significant influence of temperature distribution during printing on the relationship between sample structure and properties. Printing along the short axis was shown to enhance thermal retention, which increased crystallinity and improved mechanical strength compared to samples printed along the long axis. The tracer diffusion coefficient was determined using neutron reflectometry, which facilitated the development of a model describing diffusion as a function of time and temperature. In 2020, Talley et al. explored the static structure of porous silicone rubber and elucidated the relationship between various filler compositions (alumina, graphite, and titanium dioxide) and their mechanical response [62]. The ultra-small angle X-ray scattering (USAXS) and SAXS data obtained were analyzed by the Unified Fit model derived by Beaucage [71], which can better deal with fractal aggregates and multi-scale structural systems. The main particle size of the filling material is determined, and the process by which these particles aggregate into larger clusters is precisely captured.

In addition, SAXS provides direct data on particle aggregation and stability, which is useful for evaluating the dispersion of modified fillers in the matrix and for increasing understanding of the filler network. In 2019, Staropoli et al. carried out a microstructural study of different types of filled rubbers under quasi-static stretching using USAXS in combination with transmission electron microscopy to explore the structural changes of silica filler clusters under tilting and reverse [72]. The structural changes of silica filler clusters under tilting and reverse deformation at the hundred nanometer scale were explored, as shown in Fig. 11. They combined the proposed polydisperse pragmatic particle form factor with the fractal cluster model developed by Teixeira [73], and obtained the structure factor of aggregation. In 2023, Okoli et al. used SAXS/USAXS to study the mesostructure of filler silica and the poor filling network formed in the composite due to the presence of silanol groups on the surface [74].

5. Applications of neutron scattering technology in 3D printing of silicone rubber

Numerous studies have demonstrated that the enhanced mechanical properties of silicone rubber nanocomposites are attributed to the synergistic effects of multilevel silicone rubber structures induced by fillers [30,31], including rubber networks, filler networks, and filler-rubber networks. This indicates that the properties of silicone rubber are not solely governed by the static characteristics of the nanostructure but also intricately linked to the dynamic behavior of molecular chain segments on time scales ranging from nanoseconds to microseconds. SAXS relies primarily on changes in electron density within the material to gather structural information, while neutron scattering interacts with atomic nuclei and is particularly sensitive to hydrogen atoms, making it effective at detecting the dynamic behavior of polymer chains and phase separation phenomena. In many cases, neutron scattering techniques can be

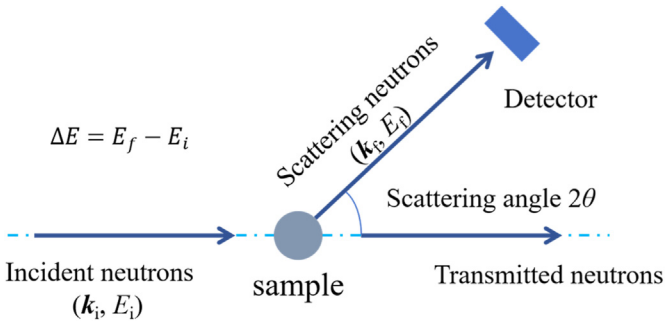

Fig. 12. Geometric diagram of neutron scattering experiment. According to the different energy transfer, there are three different interactions: (1) Elastic scattering ($\Delta E = 0$). There is no exchange of energy between the incident neutron and the particles in the sample; (2) Inelastic scattering ($|\Delta E| > 0$). There is a large, quantifiable exchange of energy between neutrons and particles; (3) Quasi-elastic scattering ($\Delta E \approx 0$).

complemented and cross-checked with SAXS to gain a more complete understanding of material properties [75,76]. The properties of neutron determine that it can be used as a probe to study the microscopic physical properties of condensed matter, and its principle is shown in Fig. 12. According to whether the neutron energy changes before and after scattering at the sample, the neutron scattering techniques can be divided into two categories: inelastic neutron scattering and elastic neutron scattering, which are suitable for detecting the micromesoscopic structure and dynamics of materials respectively.

5.1. Elastic neutron scattering

Similar to the SAXS, the intensity $I(q)$ of neutron scattering obtained from integrating the two-dimensional scattering image is measured by small-angle neutron scattering (SANS) as a function of the scattering vector q. SANS has many unique advantages specific to silicone rubber research: (1) The coherent scattering length density (SLD) of H ($SLD_H = -0.37 \times 10^{-12}$ cm) and D ($SLD_D = 0.67 \times 10^{-12}$ cm) is significantly different. The combination of neutron scattering with specified deuterium groups and structural labelling can effectively distinguish the conformational information and aggregation state information of specific components and obtain direct experimental data on the relationship between "chain conformation-condensed state-property" of the system. SANS can cover the detection range from nanometer to micrometer scale, which is very suitable for the study of nanoparticle-filled polymers at different levels of aggregation structure, interface, as well as the evolution of these microstructures and mechanical properties under the service state.

In research of silicone rubber, SANS has provided detailed insights into molecular chain arrangement, filler networks, and bound rubber (BR) structure. These microscopic features are essential for understanding the mechanical properties of silicone rubber, its internal stress distribution, and its formation during printing.

Fillers with different surface structures, geometries, and sizes facilitate the development of unique layered structures in silicone rubber systems, resulting in distinct reinforcement properties [77,78]. A substantial body of research has demonstrated that nano-filler reinforcement is an effective approach for enhancing the mechanical properties of silicone rubber, with the key role of this enhancement attributed to the interaction between the rubber and the BR phase [67]. Notably, Shui et al. utilized contrast variation-small-angle neutron scattering (CV-SANS, the principle is schematically depicted in Fig. 13), to analyze the scattering behavior of immobilized silicone rubber in a mixed solvent [79]. They configured H-toluene and D-toluene solvents in different ratios, obtained scattering functions with different liner differences, simplified the three-phase system of "silicone rubber-silica-interface" into two sets of two-phase systems, decoupled the microstructural

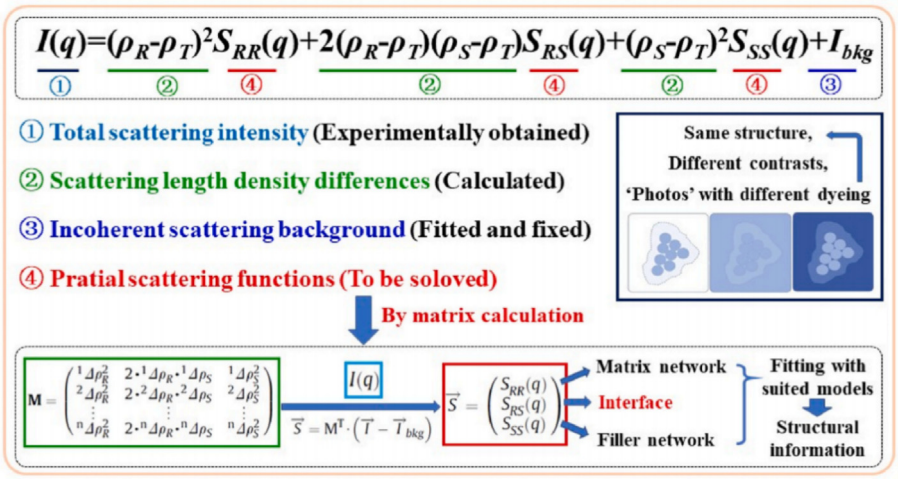

Fig. 13. Schematic diagram of CV-SANS decoupling principle [79]. Copyright 2019, Composites Science and Technology.

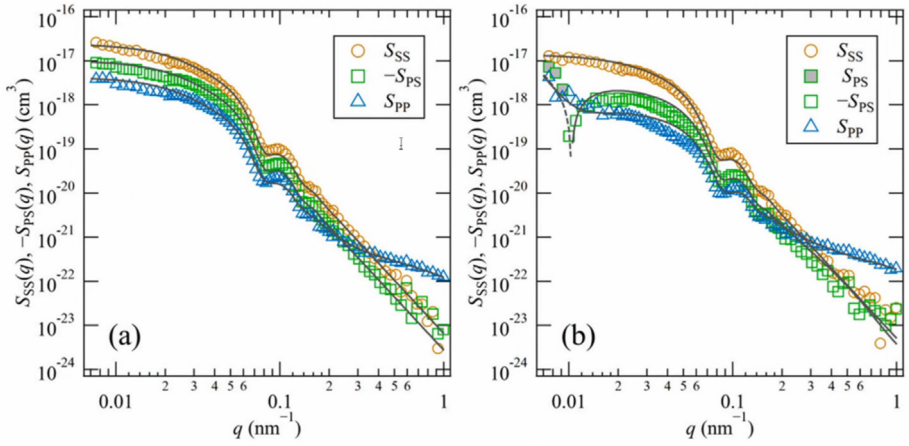

Fig. 14. Partial scattering functions of (a) A (without silane coupling agent) and (b) B (with silane coupling agent). The black lines indicate the fitting results [80]. Copyright 2024, Polymer.

information of each component, and wrote the scattering intensity function in the following form:

$$I(q) = (\rho_R - \rho_T)^2 S_{RR}(q) + 2(\rho_R - \rho_T)(\rho_S - \rho_T)S_{RS}(q) + (\rho_S - \rho_T)S_{SS}(q) + I_{bkg}$$

Where ρ_R, ρ_T, and ρ_S are the SLD of silicone rubber, toluene and silica, respectively. I_{bkg} is incoherent background. Considering the complex non-uniform distribution of aggregate fractals and particles in the system, the three partial scattering functions obtained are then fitted according to the Beaucage unified function.

In 2024, Nakanishi et al. quantitatively elucidated the thickness of the adsorbed layer and the degree of aggregation in silicone rubber systems with/without silica filler by the CV-SANS method [80]. They pointed out that in the system without silane coupling agent (denoted by A), there was no adsorption layer around the particles and the particles had a tendency to aggregate. On the other hand, an adsorption layer of about 5.3 nm was formed on the surface of the particles in the system with silane coupling agent (denoted by B), indicating that the addition of silane coupling agent suppressed the aggregation phenomenon. As shown in Fig. 14. For A, the scattering is dominated by the network structure of the polymer except in the high-q region, implying that there is no adsorption layer at the silica particle interface, thus treating the silica particles as a mixture of isolated particles and small aggregates for a two-phase model. For B, the size of the non-uniform structure based on the crosslinked network and mesh size of the network, derived from Debye-Bueche and Ornstein-Zernike-Debye equations, is considered [81]. In contrast to the Beaucage model, this method can be used to describe the agglomeration behavior of simple particle systems or particles for systems with low dispersion.

In situ SANS allows measurement of material properties in real-world application environments, such as high temperature, humidity or dynamic force loading, providing real-time observation of nanostructures evolution. It can also reveal how fillers are redistributed, oriented, or depolymerized during stretching, elucidating the evolution mechanisms of layered structures. In 2023, Han et al. studied the dynamic evolution of microstructure under Mullins loading based on *in situ* SANS technique, investigating the fatigue and damage mechanisms of the bonded layer in silicone rubber. By integrating deuterated chain labelling with *in situ* SANS techniques, they monitored the structural evolution under cyclic stretching. Fig. 15 shows that the orientation degree of the bound rubber (BR) increases with both strain and cycle number. Constitutive analysis confirmed that the differing responses of the matrix and fillers to external strain stages lead to varying degrees of BR orientation [82]. The radius of gyration of BR-coated packing agglomerates in the horizontal (R_g^H) and vertical (R_g^V) directions was obtained by fitting a one-dimensional SANS curve using the Guinier-Porod model [83].

The SANS technique can elucidate the intricate relationship between microstructure and macroscopic properties, from the distribution of

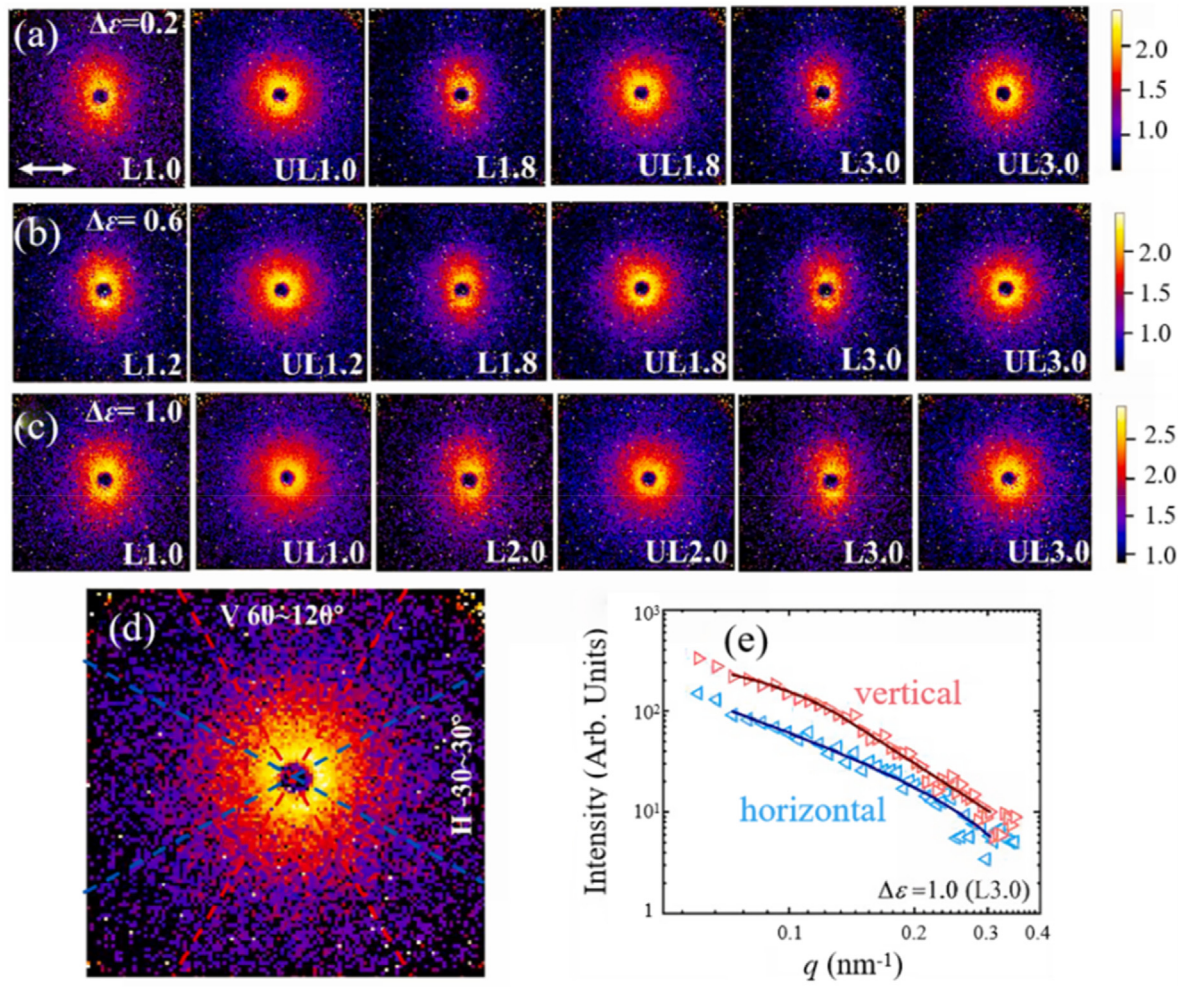

Fig. 15. SANS profiles for the BR-coated filler aggregates under cyclic strain rise path deformation. Two-dimensional SANS pattern as an example to illustrate the integration range within the first 300 s during 1.0 process of strain interval (d) and selected 2D SANS patterns with different strain during loading (L) and unloading (UL) under 0.2 (a), 0.6 (b), and 1.0 (c) processes of strain interval, respectively. Each pattern is collected within duration of 150 s before and after each given strain. (e) Selected 1D SANS profiles and the fitting results in horizontal (H) and vertical (V) directions (the range of q for fitting is 0.07–0.3 nm^{-1}) [81]. Copyright 2023, Composites: Part A.

fillers to the evolution of layered structures, which makes it an invaluable tool for the design optimization of silicone rubber materials.

5.2. *Quasi-elastic neutron scattering*

High-resolution inelastic neutron scattering (INS) techniques, such as neutron quasi-elastic scattering (QENS) and neutron spin echo (NSE), offer effective means to directly probe the internal dynamic behavior and molecular motion of polymers. By measuring the energy transfer of scattered neutrons, these methods enable detailed analysis of local molecular motions, diffusion behavior, and interactions within the internal chains of materials over a broad timescale range (0.1–100 ns) [84]. QENS is particularly well-suited for investigating high-frequency, short-range local motions, such as the segmental jumping motions of polymer chains and molecular diffusion [85]. In contrast, NSE is an efficient tool for exploring the dynamics of intermediate polymers in polymer nanocomposites (PNC) [75,86], enabling the direct measurement of the Intermediate Scattering Function (ISF) or $I(q, t)$, which provides insights into the various modes of motion within polymer systems.

In 1971, Allen et al. studied PDMS by QENS technique, revealing persistent Doppler broadening in low molecular weight liquids, high molecular weight gums, and even cross-linked rubbers [87]. In 1999, Arrighi et al. investigated the influence of fillers on the fast segment dynamics of polymers using QENS, demonstrating that the presence of filler particles constrained polymer chain mobility. Their findings identified two distinct dynamic processes: one involving freely diffusing chains and the other highly constrained chains [88]. However, due to the semi-crystalline nature of PDMS, the dynamics associated with loose chains, which are responsible for the second glass transition, could not be detected. Furthermore, the presence of nanoparticles has been shown to alter the dynamic behavior of polymer chains.

In experimental investigations, the Rouse model is commonly employed to describe the relaxation dynamics of chain segments in non-entangled polymer melts over a relatively short time scale. However, beyond the timescale and spatial window defined by the Rouse model, the dynamics of long polymer chains become constrained by topological entanglements. In the reptation model, polymer chains are restricted by a "pipeline" and move in a serpentine fashion within its confines. NSE spectroscopy has proven to be an ideal tool for investigating both entropy-driven Rouse dynamics and reptation motion at intermediate length scales [89,90]. The measurements are usually normalized at t = 0,

$$\frac{I(q,t)}{I(q,0)} = \frac{p(q,t)}{P(q,0)}$$

Where $P(q)$ is the form factor of the polymer chain and describes the collective motion of the monomers in the polymer chain. The decay of this function with time reveals the relaxation dynamics of the polymer

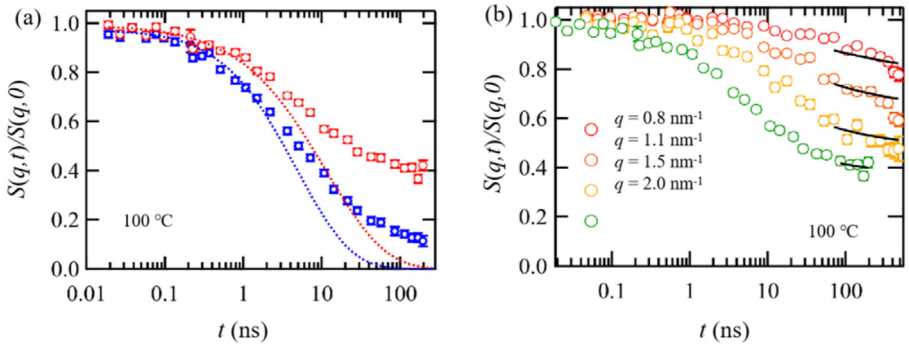

Fig. 16. (a) $S(q,t)/S(q,0)$ of the bound (red hollow symbol) and free (blue hollow symbol) chains and their corresponding Rouse model fit at 100 °C and $q = 2.0$ nm^{-1} is shown. (b) $S(q,t)/S(q,0)$BR for the BR-coated CB in dPB at the given four q values and 100 °C. The solid lines correspond to the best fit of the reptation model to the data [91]. Copyright 2021, Macromolecules.

Table 1
Comparison of characterization techniques of scattering methods.

Techniques	Information	Scale range	Advantages	Limitations
SAXS USAXS	Multiscale structures	1–100 nm 100 nm–10 μm	Non-destructive; sensitive to electron cloud density; *in situ* studies	Risk of adiation damage
SANS		1 nm–600 nm	Non-destructive;	Time-consuming
QENS NSE	Relaxation processes	10^{-13}–10^{-7} s 10^{-1}–10^{-6} s; 0.6–600 nm	sensitive to light elements and isotopes; *in situ* studies	Time-consuming; limited availability; sample deuteration required

chain under the corresponding scattering vector q.

In 2021, Salatto et al. conducted an investigation on spherical carbon black-filled, monodisperse polybutadiene (PB) systems, using the NSE technique in combination with neutron-specific contrast matching techniques to selectively probe the behavior of BR chains [91]. The experimental data and fitting results of NSE are shown in Fig. 16a, which can explain the initial relaxation well, and the resulting deviations are attributed to local compensation. Therefore, they applied a two-phase model to the NSE data and used the reptation model to analyze the tube diameter of the BR:

$$\frac{S(q,t)}{S(q,0)} = \mu + (1-\mu)\left[1 - \exp\left(-\frac{q^2d^2}{36}\right)\right] S_{local}(q,t) + \exp\left(-\frac{q^2d^2}{36}\right) S_{esc}(q,t)$$

Where μ is the fraction of immobile polymer on the fillers' surface, $S_{local}(q,t)$ and $S_{esc}(q,t)$ represent the local Rouse motion along the tube and the contribution of escaping from tube, respectively. The experimental data and fitting results of NSE are shown in Fig. 16b. In the time window of NSE, the chain does not escape, so $S_{esc}(q,t) = 1$ and they fits the data under the corresponding relaxation window. By quantitatively isolating the contributions from ring and tail chains, their study demonstrated that tail-tail chain interactions have a negligible effect on the physical adsorption of chains. Furthermore, through the integration of molecular dynamics simulations, their work provided new insights into the local structure and dynamic heterogeneity of BR chains, as well as their interactions with the matrix polymer. In 2022, Philippe et al. studied the structure and dynamics of industrial rubber materials filled with silica-polyisoprene composites [92]. Using both SANS and NSE, they identified a unique polymer chain population exhibiting distinct dynamic behavior at the packing surface. Their findings indicated that the addition of fillers did not significantly alter the dynamic behavior of chain relaxation in response to temperature changes.

During the 3D printing process, silicone rubber undergoes shear stress and curing, leading to more complex molecular dynamics. Traditional static analysis methods are insufficient to capture these intricate dynamic processes. By offering high temporal and spatial resolution, QENS and NSE techniques provide valuable insights into both local and large-scale dynamics of silicone rubber chain segments. These techniques can facilitate the optimization of processing parameters such as temperature, speed, and pressure during printing, thereby ensuring material homogeneity and enhancing interlayer adhesion. The characteristics and comparisons of different scattering techniques are presented in Table 1.

6. Conclusions and outlook

With rapid advancements in 3D printing technologies, silicone rubber, renowned for its exceptional flexibility, weather resistance, and biocompatibility, has shown considerable potential for applications across various fields, including medical devices, flexible electronics, soft robotics, and high-performance seals. However, current research on 3D printed silicone rubber still faces several challenges. Notably, the high viscosity and slow curing rate of silicone rubber significantly constrain its printing accuracy and efficiency. Moreover, the incorporation of fillers, the formation of interlayer interfaces during the printing process, and the dynamic reorganization of materials under external stimuli substantially influence the mechanical properties, toughness, and fatigue resistance of silicone rubber.

The microstructure, interfacial properties, and dynamic behavior of materials are pivotal in determining their macroscopic properties and functional performance. Traditional characterization techniques, such as optical microscopy, electron microscopy, and thermal analysis, are insufficient for nanoscale structural investigations. In this context, neutron scattering techniques offer significant promise due to their unique advantages in probing material structures at the atomic and nanoscopic levels. The spin-echo small-angle neutron scattering (SESANS) technique, an extension of SANS based on the neutron spin echo effect, quantifies the spin and polarization precession of scattered neutrons under the influence of magnetic fields to obtain scattering angle information. SESANS offers superior resolution and the ability to conduct measurements over a larger scale (10 nm–10 μm) [93–95]. Leveraging the advantages of SESANS, such as micron-scale detection, easy processing of multiple scattering, and reduced interference from incoherent scattering, it provides a powerful approach to investigating the filler networks in filled rubbers. When coupled with the unique contrast variation capabilities of neutron scattering, SESANS is expected to significantly advance the study of structural characteristics, particularly in relation to the interfacial adhesive layers within filler networks.

The development of functionalized silicone rubber materials remains

a critical focus for future research. By incorporating conductive fillers, magnetic particles, or stimuli-responsive materials, silicone rubber can be endowed with additional functionalities, such as electrical conductivity, self-healing properties, or intelligent responsiveness. These functionalized materials are expected to accelerate the broader adoption of 3D printed silicone rubber in flexible electronics, wearable devices, and smart sensors. In parallel, as 3D printing technologies continue to mature and gain widespread application in silicone rubber research, 4D printing, i.e., an emerging technique, has garnered increasing attention. By integrating the time dimension into the 3D printing process, 4D printing enables the printed silicone rubber to undergo shape morphing, performance modulation, and even structural reconfiguration in response to external stimuli (e.g., temperature, humidity, electric or magnetic fields, or light). This approach unlocks new avenues for more functional and intelligent applications [96]. The integration of 4D printing technologies will facilitate the transition of silicone rubber materials from static structures to dynamic, adaptable, and multifunctional configurations.

CRediT authorship contribution statement

Xiang Luo: Writing – original draft, Investigation, Conceptualization. **Shengyi Zhong:** Writing – review & editing, Investigation, Funding acquisition. **Dong Liu:** Writing – review & editing, Supervision, Resources, Methodology, Investigation, Conceptualization.

Declaration of competing interest

The authors declare that they have no known competing financial interests or personal relationships that could have appeared to influence the work reported in this paper.

Acknowledgments

This work was supported by the National Key Research and Development Program of China (Grant No. 2021YFA1600900), the National Natural Science Foundation of China (Grant Nos. 12275248 and U21A2090), Central Guidance for Local Science and Technology Development Fund Project (Grant Nos. 2023ZYDF098 and 2023ZYDF075), and Innovation and Development Fund of CAEP (Grant No. CXKS20240052). The research is also in part supported by “Ludo Frevel Crystallography Scholarships” (D. Liu, 2015) from the International Centre for Diffraction Data (ICDD). D. Liu acknowledges the experts and beamtime support of CSNS, CARR, SSRF, NSRL, and BSRF.

References

[1] S.C. Ligon, et al., Polymers for 3D printing and customized additive manufacturing, Chem. Rev. 117 (2017) 10212–10290, https://doi.org/10.1021/acs.chemrev.7b00074.
[2] G. Postiglione, et al., Conductive 3D microstructures by direct 3D printing of polymer/carbon nanotube nanocomposites via liquid deposition modeling, Compos. Appl. Sci. Manuf. 76 (2015) 110–114, https://doi.org/10.1016/j.compositesa.2015.05.014.
[3] A. Della Bona, et al., 3D printing restorative materials using a stereolithographic technique: a systematic review, Dent. Mater. 37 (2021) 336–350, https://doi.org/10.1016/j.dental.2020.11.030.
[4] D.D. Gu, et al., Laser additive manufacturing of metallic components: materials, processes and mechanisms, Int. Mater. Rev. 57 (2012) 133–164, https://doi.org/10.1179/1743280411Y.0000000014.
[5] R.D. Murphy, et al., Tailored polypeptide star copolymers for 3D printing of bacterial composites via direct ink writing, Adv. Mater. 35 (2023) 2207542, https://doi.org/10.1002/adma.202207542.
[6] C. Ioannidou, et al., In-situ synchrotron X-ray analysis of metal Additive Manufacturing: current state, opportunities and challenges, Mater. Des. 219 (2022) 110790, https://doi.org/10.1016/j.matdes.2022.110790.
[7] C. Buchanan, L. Gardner, Metal 3D printing in construction: a review of methods, research, applications, opportunities and challenges, Adv. Funct. Mater. 180 (2019) 332–348, https://doi.org/10.1016/j.engstruct.2018.11.045.
[8] L.Y. Zhou, J. Fu, Y. He, A review of 3D printing technologies for soft polymer materials, Adv. Funct. Mater. 30 (2020) 2000187, https://doi.org/10.1002/adfm.202000187.
[9] R.S. Jordan, et al., 3D printed architected conducting polymer hydrogels, J. Mater. Chem. B 9 (2021) 7258–7270, https://doi.org/10.1039/d1tb00877c.
[10] J.W. Kemp, et al., Direct ink writing of ZrB2-SiC chopped fiber ceramic composites, Addit. Manuf. 44 (2021) 102049, https://doi.org/10.1016/j.addma.2021.102049.
[11] Y. Zhao, et al., 3D printing of unsupported multi-scale and large-span ceramic via near-infrared assisted direct ink writing, Nat. Commun. 14 (2023) 2381, https://doi.org/10.1038/s41467-023-38082-8.
[12] J. Xiao, et al., Large-scale 3D printing concrete technology: current status and future opportunities, Cem. Concr. Compos. 122 (2021) 104115, https://doi.org/10.1016/j.cemconcomp.2021.104115.
[13] S. Muthukrishnan, S. Ramakrishnan, J. Sanjayan, Technologies for improving buildability in 3D concrete printing, Cement Concr. Compos. 122 (2021) 104144, https://doi.org/10.1016/j.cemconcomp.2021.104144.
[14] T. Thomas, et al., Extrusion 3D printing of porous silicone architectures for engineering human cardiomyocyte-infused patches mimicking adult heart stiffness, ACS Appl. Bio Mater. 3 (2020) 5865–5871, https://doi.org/10.1021/acsabm.0c00572.
[15] S. Duraivel, D. Laurent, et al., A silicone-based support material eliminates interfacial instabilities in 3D silicone printing, Science 379 (2023) 1248–1252, https://doi.org/10.1126/science.ade4441.
[16] K. Yu, A. Xin, et al., Additive manufacturing of self-healing elastomers, NPG Asia Mater. 11 (2019) 7, https://doi.org/10.1038/s41427-019-0109-y.
[17] Z. Wang, et al., 3D printable silicone rubber for long-lasting and weather-resistant wearable devices, ACS Appl. Polym. Mater. 4 (2022) 2384–2392, https://doi.org/10.1021/acsapm.1c01674.
[18] S.O. Catt, et al., Macromolecular engineering: from precise macromolecular inks to 3D printed microstructures, Small 19 (2023) 2300844, https://doi.org/10.1002/smll.202300844.
[19] M. Zarek, et al., 3D printing of shape memory polymers for flexible electronic devices, Adv. Mater. 28 (2015) 4449–4454, https://doi.org/10.1002/adma.201503132.
[20] S. Peng, et al., 3D printing mechanically robust and transparent polyurethane elastomers for stretchable electronic sensors, ACS Appl. Mater. Interfaces 12 (2020) 6479–6488, https://doi.org/10.1021/acsami.9b20631.
[21] Z. Weng, et al., 3D printing of ultra-high viscosity resin by a linear scan-based vat photopolymerization system, Nat. Commun. 14 (2023) 4303, https://doi.org/10.1038/s41467-023-39913-4.
[22] G. Wei, et al., Solvent-free high-performance photocurable 3D printing resin from a noncoplanar branched maleimide oligomer for high-resolution fabrication, Addit. Manuf. 79 (2024) 103924, https://doi.org/10.1016/j.addma.2023.103924.
[23] S. Goyal, A. Yesu, S.S. Banerjee, Direct ink writing-based additive manufacturing of styrene-isoprene-styrene block copolymer, Polym. Eng. Sci. 63 (2023) 3708–3718, https://doi.org/10.1002/pen.26478.
[24] M. Kim, et al., 3D printable modular soft elastomers from physically cross-linked homogeneous associative polymers, ACS Polym. Au 4 (2024) 98–108, https://doi.org/10.1021/acspolymersau.3c00021.
[25] L.Y. Wong, S. Ganguly, X.S. Tang, 3D vat photopolymerization printing of hydrophilic silicone-based microfluidic devices and the effect of cellulose nanocrystals as additives for improved printing accuracy, Addit. Manuf. 86 (2024) 104177, https://doi.org/10.1016/j.addma.2024.104177.
[26] X. Xu, et al., 3D printing of high-strength silicone-based polyurethane-polyurea enabled by growth of covalent cross-linked network, Chem. Eng. J. 488 (2024) 150810, https://doi.org/10.1016/j.cej.2024.150810.
[27] V.J. Garcia, et al., On the direct ink write (DIW) 3D printing of styrene-butadiene rubber (SBR)-based adhesive sealant, MRS Commun 13 (2023) 1266–1274, https://doi.org/10.1557/s43579-023-00436-0.
[28] J.R. Potts, et al., Graphene-based polymer nanocomposites, Polymer 52 (2011) 5–25, https://doi.org/10.1016/j.polymer.2010.11.042.
[29] X. Sun, et al., Recent progress in graphene/polymer nanocomposites, Adv. Mater. 33 (2020) 2001105, https://doi.org/10.1002/adma.202001105.
[30] Y. Xu, et al., Effects of functional graphene oxide on the properties of phenyl silicone rubber composites, Polym. Test. 54 (2016) 168–175, https://doi.org/10.1016/j.polymertesting.2016.07.013.
[31] Q. Chen, et al., 3D printed multifunctional, hyperelastic silicone rubber foam, Adv. Funct. Mater. 29 (2019) 1900469, https://doi.org/10.1002/adfm.201900469.
[32] D.A. Porter, et al., Additive manufacturing with ultraviolet curable silicones containing carbon black, 3D Printing Addit. Manufact. 5 (2018) 73–86, https://doi.org/10.1089/3dp.2017.0019.
[33] J. Wang, et al., Selective laser sintering of polydimethylsiloxane composites, 3D Print, Addit. Manuf. 10 (2021) 684–696, https://doi.org/10.1089/3dp.2021.0105.
[34] M.M. Durban, et al., Custom 3D printable silicones with tunable stiffness, Macromol. Rapid Commun. 39 (2018) 1700563, https://doi.org/10.1002/marc.201700563.
[35] F.D.C. Siacor, et al., On the additive manufacturing (3D printing) of viscoelastic materials and flow behavior: from composites to food manufacturing, Addit. Manuf. 45 (2021) 102043, https://doi.org/10.1016/j.addma.2021.102043.
[36] T.J. Ober, D. Foresti, J.A. Lewis, Active mixing of complex fluids at the microscale, Proc. Natl. Acad. Sci. USA. 112 (2015) 12293–12298, https://doi.org/10.1073/pnas.1509224112.

[37] L.-y. Zhou, et al., Multimaterial 3D printing of highly stretchable silicone elastomers, ACS Appl. Mater. Interfaces 11 (2019) 23573–23583, https://doi.org/10.1021/acsami.9b04873.
[38] R.L. Truby, J.A. Lewis, Printing soft matter in three dimensions, Nature 540 (2016) 371–378, https://doi.org/10.1038/nature21003.
[39] C. Geng, et al., 3D Printed Architectured silicone composites containing a UV-curable rheological modifier with tailorable structural collapse, Compos. Part B: Eng. 280 (2024) 111490.
[40] S. Zheng, et al., Multiple modulus silicone elastomers using 3D extrusion printing of low viscosity inks, Addit. Manuf. 24 (2018) 86–92, https://doi.org/10.1016/j.addma.2018.09.011.
[41] A. Leonov, Analysis of simple constitutive equations for viscoelastic liquids, J. Non-Newton. Fluid Mech. 42 (1992) 323–350, https://doi.org/10.1016/0377-0257(92)87017-6.
[42] K. Sahu, et al., Linear instability of pressure-driven channel flow of a Newtonian and a Herschel-Bulkley fluid, Phys. Fluids 19 (2007), https://doi.org/10.1063/1.2814385.
[43] Y. Shao, et al., Study on ink flow of silicone rubber for direct ink writing, J. Appl. Polym. Sci. 138 (2021) 50819, https://doi.org/10.1002/app.50819.
[44] J. Stieghorst, T. Doll, Rheological behavior of PDMS silicone rubber for 3D printing of medical implants, Addit. Manuf. 24 (2018) 217–223, https://doi.org/10.1016/j.addma.2018.10.004.
[45] D.K. Patel, et al., Highly stretchable and UV curable elastomers for digital light processing based 3D printing, Adv. Mater. 29 (2017) 1606000, https://doi.org/10.1002/adma.201606000.
[46] Z. Ding, et al., Ultraviolet-assisted material extrusion of silicones with largely enhanced mechanical properties and isotropy, Addit. Manuf. 80 (2024) 103965, https://doi.org/10.1016/j.addma.2024.103965.
[47] R. Woo, et al., Structure–mechanical property relationships of 3D-printed porous polydimethylsiloxane, ACS Appl. Polym. Mater. 3 (2021) 3496–3503, https://doi.org/10.1021/acsapm.1c00417.
[48] G. Tsagaropoulos, A. Eisenberg, Dynamic mechanical study of the factors affecting the two glass transition behavior of filled polymers. Similarities and differences with random ionomers, Macromolecules 28 (1995) 6067–6077, https://doi.org/10.1021/ma00122a011.
[49] V.M. Miron, et al., Material characterization of 3d-printed silicone elastomers, Procedia Struct. Integr. 34 (2021) 65–70, https://doi.org/10.1016/j.prostr.2021.12.010.
[50] E.B. Duoss, et al., Three-dimensional printing of elastomeric, cellular architectures with negative stiffness, Adv. Funct. Mater. 24 (2014) 4905–4913, https://doi.org/10.1002/adfm.201400451.
[51] X. Zhu, et al., Stress relaxation behavior of 3D printed silicone rubber foams with different topologies under uniaxial compressive load, Compos. Commun. 38 (2023) 101475, https://doi.org/10.1016/j.coco.2022.101475.
[52] B.G. Compton, J. Lewis, 3D-printing of lightweight cellular composites, Adv. Mater. 26 (2014) 5930–5935, https://doi.org/10.1002/adma.201401804.
[53] S.Y. Baraki, et al., Regenerated chitin reinforced polyhydroxybutyrate composites via Pickering emulsion template with improved rheological, thermal, and mechanical properties, Compos. Commun. 25 (2021) 100655, https://doi.org/10.1016/j.coco.2021.100655.
[54] O.J. Aryeetey, et al., Development of 3D printed tissue-mimicking materials: combining fiber reinforcement and fluid content for improved surgical rehearsal, Materialia (Oxf) 34 (2024) 102088, https://doi.org/10.1016/j.mtla.2024.102088.
[55] P. Huang, Z. Xia, S. Cui, 3D printing of carbon fiber-filled conductive silicon rubber, Mater. Des. 142 (2018) 11–21, https://doi.org/10.1016/j.matdes.2017.12.051.
[56] M.-J. Wang, The role of filler networking in dynamic properties of filled rubber, Rubber Chem. Technol. 72 (1999) 430–448, https://doi.org/10.5254/1.3538812.
[57] A. Sircar, et al., Glass transition of elastomers using thermal analysis techniques, Rubber Chem. Technol. 72 (1999) 513–552, https://doi.org/10.5254/1.3538816.
[58] Q. Xu, et al., Mechanical properties of silicone rubber composed of diverse vinyl content silicone gums blending, Mater. Des. 31 (2010) 4083–4087, https://doi.org/10.1016/j.matdes.2010.04.052.
[59] M. Schaffner, et al., 3D printing of robotic soft actuators with programmable bioinspired architectures, Nat. Commun. 9 (2018) 878, https://doi.org/10.1038/s41467-018-03216-w.
[60] X. Zhu, et al., Structure–mechanical property relationships of 3D-printed porous polydimethylsiloxane films, Nanotechnol. Rev. 12 (2023) 20230188, https://doi.org/10.1515/ntrev-2023-0188.
[61] L. Huang, et al., Structural analyses of the bound rubber in silica-filled silicone rubber nanocomposites reveal mechanisms of filler-rubber interaction, Compos. Sci. Technol. 233 (2023) 109905, https://doi.org/10.1016/j.compscitech.2022.109905.
[62] S.J. Talley, et al., Impact of filler composition on mechanical and dynamic response of 3-D printed silicone-based nanocomposite elastomers, Compos. Sci. Technol. 198 (2020) 108258, https://doi.org/10.1016/j.compscitech.2020.108258.
[63] D. Ciprari, K. Jacob, R. Tannenbaum, Characterization of polymer nanocomposite interphase and its impact on mechanical properties, Macromolecules 39 (2006) 6565–6573, https://doi.org/10.1021/ma0602270.
[64] A. Grard, L. Belec, F. Perrin, Effect of surface morphology on the adhesion of silicone elastomers on AA6061 aluminum alloy, Int. J. Adhes. Adhesives 102 (2020) 102656, https://doi.org/10.1016/j.ijadhadh.2020.102656.
[65] A. Foerster, et al., UV-curable silicone materials with tuneable mechanical properties for 3D printing, Mater. Des. 205 (2021) 109681, https://doi.org/10.1016/j.matdes.2021.109681.
[66] S. Walker, et al., Predicting interfacial layer adhesion strength in 3D printable silicone, Addit. Manuf. 47 (2021) 102320, https://doi.org/10.1016/j.addma.2021.102320.
[67] N. Jouault, et al., Bound polymer layer in nanocomposites, ACS Macro Lett. 2 (2013) 371–374, https://doi.org/10.1021/mz300646a.
[68] L. Xia, et al., Silica nanoparticles reinforced natural rubber latex composites: the effects of silica dimension and polydispersity on performance, J. Appl. Polym. Sci. 136 (2019) 47449, https://doi.org/10.1002/app.47449.
[69] T. Li, A.J. Senesi, B. Lee, Small angle X-ray scattering for nanoparticle research, Chem. Rev. 116 (2016) 11128–11180, https://doi.org/10.1021/acs.chemrev.5b00690.
[70] Y. Shmueli, et al., Simultaneous in situ X-ray scattering and infrared imaging of polymer extrusion in additive manufacturing, ACS Appl. Polym. Mater. 1 (2019) 1559–1567, https://doi.org/10.1021/acsapm.9b00328.
[71] G. Beaucage, D.W. Schaefer, Structural studies of complex systems using small-angle scattering: a unified guinier/power-law approach, J. Non-Cryst. Solids 172 (1994) 797–805, https://doi.org/10.1016/0022-3093(94)90581-9.
[72] M. Staropoli, D. Gerstner, et al., Hierarchical scattering function for silica-filled rubbers under deformation: effect of the initial cluster distribution, Macromolecules 52 (2019) 9735–9745, https://doi.org/10.1021/acs.macromol.9b01751.
[73] J. Teixeira, Small-angle scattering by fractal systems, J. Appl. Crystallogr. 21 (1988) 781–785, https://doi.org/10.1107/S0021889888000263.
[74] U. Okoli, K. Rishi, et al., Dispersion of modified fumed silica in elastomeric nanocomposites, Polymer 264 (2023) 125407, https://doi.org/10.1016/j.polymer.2022.125407.
[75] F. Spinozzi, et al., Structural and thermodynamic properties of nanoparticle–protein complexes: a combined SAXS and SANS study, Langmuir 33 (2017) 2248–2256, https://doi.org/10.1021/acs.langmuir.6b04072.
[76] N. Jouault, et al., Direct measurement of polymer chain conformation in well-controlled model nanocomposites by combining SANS and SAXS, Macromolecules 43 (2010) 9881–9891, https://doi.org/10.1021/ma101682t;
[75] E.J. Bailey, K.I. Winey, Dynamics of polymer segments, polymer chains, and nanoparticles in polymer nanocomposite melts: a review, Prog. Polym. Sci. 105 (2020) 101242, https://doi.org/10.1016/j.progpolymsci.2020.101242.
[77] L.-Z. Huang, et al., How the aggregates determine bound rubber models in silicone rubber? A contrast matching neutron scattering study, Chin. J. Polym. Sci. 39 (2021) 365–376, https://doi.org/10.1007/s10118-020-2485-8.
[78] L.-Z. Huang, et al., Effects of various filler surfaces on tuning the hierarchical structures and reinforcement of silicone rubbers, Surf. Interfaces 41 (2023) 103254, https://doi.org/10.1016/j.surfin.2023.103254.
[79] Y. Shui, L. Huang, et al., How the silica determines properties of filled silicone rubber by the formation of filler networking and bound rubber, Compos. Sci. Technol. 215 (2021) 109024, https://doi.org/10.1016/j.compscitech.2021.109024.
[80] Y. Nakanishi, M. Shibata, et al., Analyses of hierarchical structures in SBR rubber by using contrast-variation SANS: effects of a silane coupling agent, Polymer 306 (2024) 127209, https://doi.org/10.1016/j.polymer.2024.127209.
[81] Y. Ikeda, N. Higashitani, et al., Vulcanization: new focus on a traditional technology by small-angle neutron scattering, Macromolecules 42 (2009) 2741–2748, https://doi.org/10.1021/ma802730z.
[82] J.-J. Han, et al., The maximum-strain and strain-interval dependences of microstructural evolution underneath the Mullins effect, Compos. Appl. Sci. Manuf. 172 (2023) 107586, https://doi.org/10.1016/j.compositesa.2023.107586.
[83] B. Hammouda, A new Guinier–Porod model, J. Appl. Cryst. 43 (2010) 716–719, https://doi.org/10.1107/S0021889810015773.
[84] X. Luo, T. Cui, X. Chu, Applications of neutron spin echo in soft matter, Front. Phys. 11 (2023) 1279007, https://doi.org/10.3389/fphy.2023.1279007.
[85] M. Bée, Localized and long-range diffusion in condensed matter: state of the art of QENS studies and future prospects, Chem. Phys. 292 (2003) 121–141, https://doi.org/10.1016/S0301-0104(03)00257-X.
[86] T. Wang, D. Liu, X. Du, Recent progress in elastic and inelastic neutron scattering for chemical, polymeric, and biological investigations, Curr. Opinion Solid State Mater. Sci. 31 (2024) 101175, https://doi.org/10.1016/j.cossms.2024.101175.
[87] G. Allen, et al., Motional broadening of the quasi-elastic peak in neutrons scattered from polymeric materials, Faraday Symp, Chem. Soc. 6 (1972) 169–175, https://doi.org/10.1039/FS9720600169.
[88] V. Arrighi, et al., Local dynamics of poly(dimethyl siloxane) in the presence of reinforcing filler particles, Polymer 39 (1998) 6369–6376, https://doi.org/10.1016/S0032-3861(98)00139-6.
[89] M. Krutyeva, et al., Effect of nanoconfinement on polymer dynamics: surface layers and interphases, Phys. Rev. Lett. 110 (2013) 108303, https://doi.org/10.1103/PhysRevLett.110.108303.
[90] D. Richter, M. Kruteva, Polymer dynamics under confinement, Soft Matter 15 (2019) 7316–7349, https://doi.org/10.1039/C9SM01141B.
[91] D. Salatto, et al., Structural and dynamical roles of bound polymer chains in rubber reinforcement, Macromolecules 54 (2021) 11032–11046, https://doi.org/10.1021/acs.macromol.1c01239.
[92] A.-M. Philippe, et al., Quantifying structure and dynamics of bound and bulk polymer in tailor-made rubber-silica nanocomposites, Front. Phys. 10 (2022) 1023234, https://doi.org/10.3389/fphy.2022.1023234.
[93] L. Tiihonen, et al., Revealing microscale bulk structures in polymer–carbon nanocomposites using spin-echo SANS, Soft Matter 20 (2024) 8663–8674, https://doi.org/10.1039/D4SM00578C.

[94] M.T. Rekveldt, Novel SANS instrument using neutron spin echo, Nucl. Instrum. Methods Phys. Res., Sect. A B114 (1996) 366–370, https://doi.org/10.1016/0168-583X(96)00213-3.
[95] T. Wang, et al., Design and simulations of spin-echo small angle neutron scattering spectrometer at CMRR, Nucl. Instrum. Methods Phys. Res., Sect. A 1024 (2022) 166041, https://doi.org/10.1016/j.nima.2021.166041.
[96] H. Jiang, et al., 4D printing of liquid crystal elastomer composites with continuous fiber reinforcement, Nat. Commun. 15 (2024) 8491, https://doi.org/10.1038/s41467-024-52716-5.